



## 저작자표시-비영리-변경금지 2.0 대한민국

이용자는 아래의 조건을 따르는 경우에 한하여 자유롭게

- 이 저작물을 복제, 배포, 전송, 전시, 공연 및 방송할 수 있습니다.

다음과 같은 조건을 따라야 합니다:



저작자표시. 귀하는 원저작자를 표시하여야 합니다.



비영리. 귀하는 이 저작물을 영리 목적으로 이용할 수 없습니다.



변경금지. 귀하는 이 저작물을 개작, 변형 또는 가공할 수 없습니다.

- 귀하는, 이 저작물의 재이용이나 배포의 경우, 이 저작물에 적용된 이용허락조건을 명확하게 나타내어야 합니다.
- 저작권자로부터 별도의 허가를 받으면 이러한 조건들은 적용되지 않습니다.

저작권법에 따른 이용자의 권리는 위의 내용에 의하여 영향을 받지 않습니다.

이것은 [이용허락규약\(Legal Code\)](#)을 이해하기 쉽게 요약한 것입니다.

[Disclaimer](#)

Master's Thesis  
석사학위논문

Effects of alkali carbonate additives and solvent  
composition on the electrochemical performances of  
 $\text{LiNi}_{0.5}\text{Mn}_{1.5}\text{O}_4$  cathode for lithium-ion batteries

Jung-Su Son (손 정 수 孫 廷 秀)

Department of Energy Systems Engineering  
에너지시스템공학전공

**DGIST**

**2015**

Master's Thesis  
석사학위논문

Effects of alkali carbonate additives and solvent  
composition on the electrochemical performances of  
 $\text{LiNi}_{0.5}\text{Mn}_{1.5}\text{O}_4$  cathode for lithium-ion batteries

Jung-Su Son (손 정 수 孫 廷 秀)

Department of Energy Systems Engineering  
에너지시스템공학전공

**DGIST**

**2015**

# Effects of alkali carbonate additives and solvent composition on the electrochemical performances of $\text{LiNi}_{0.5}\text{Mn}_{1.5}\text{O}_4$ cathode for lithium-ion batteries

Advisor : Professor 이 호 춘

Co-Advisor : Professor 정 낙 천

by

손정수

Department of Energy Systems Engineering

DGIST

A thesis submitted to the faculty of DGIST in partial fulfillment of the requirements for the degree of Master of Science in the Department of Energy Systems Engineering. The study was conducted in accordance with Code of Research Ethics<sup>1</sup>

05. 28. 2015

Approved by

Professor 이 호 춘 \_\_\_\_\_ ( Signature )  
(Advisor)

Professor 정 낙 천 \_\_\_\_\_ ( Signature )  
(Co-Advisor)

---

<sup>1</sup> Declaration of Ethical Conduct in Research: I, as a graduate student of DGIST, hereby declare that I have not committed any acts that may damage the credibility of my research. These include, but are not limited to: falsification, thesis written by someone else, distortion of research findings or plagiarism. I affirm that my thesis contains honest conclusions based on my own careful research under the guidance of my thesis advisor.

Effects of alkali carbonate additives and solvent composition on the electrochemical performances of  $\text{LiNi}_{0.5}\text{Mn}_{1.5}\text{O}_4$  cathode for lithium-ion batteries

손 정 수

Accepted in partial fulfillment of the requirements for the degree of  
Master of Science.

05. 28. 2015

Head of Committee \_\_\_\_\_(인)

Prof. 이호춘

Committee Member \_\_\_\_\_(인)

Prof. 정낙천

Committee Member \_\_\_\_\_(인)

Prof. 홍승태

MS/ES

201324014

손정수. Jung-Su Son. Effects of alkali carbonate additives and solvent composition on the electrochemical performances of  $\text{LiNi}_{0.5}\text{Mn}_{1.5}\text{O}_4$  cathode for lithium-ion batteries. 2015. 37p. Advisors Prof. Hochun Lee, Co-Advisors Prof. NakCheon Jeong.

### ABSTRACT

$\text{LiNi}_{0.5}\text{Mn}_{1.5}\text{O}_4$  (LNMO) is a promising and attractive cathode material due to its high operating voltage, low cost and reasonable capacity. However, the stability issue of electrolytes decomposition under the high operating voltage remains a major hurdle to its wide use. In this study, two approaches are tried to address this problem. In the first place, alkali carbonates including  $\text{CaCO}_3$ ,  $\text{MgCO}_3$ , and  $\text{Li}_2\text{CO}_3$  were employed as an electrolyte and electrode additives. It is revealed that  $\text{CaCO}_3$  as an electrode and electrolyte additive greatly improves the cycle performances at 25 °C and 55 °C and self-discharge behavior at 60 °C, which is ascribed to the HF scavenging effect of  $\text{CaCO}_3$ . The surface of the LNMO electrode after electrochemical cycling is analyzed by X-ray photoelectron spectroscopy (XPS), and the HF scavenging effect of alkali carbonates was verified by cyclic voltammetry (CV) analysis. Second, the effects of the type of the linear carbonates (LC: DMC, DEC, EMC) in 1 M  $\text{LiPF}_6$  EC/LC (3/7, v/v) are investigated. It is found that the LNMO cells with EC/DMC exhibits superior cyclability and coulombic efficiency at 25 °C and 55 °C than those with EC/EMC and EC/DEC. The cells with EC/DMC also show better self-discharge performance than other compositions. The improved electrochemical performances in EC/DMC are attributed to the diminished HF formation compared to the others.

Keywords: Li-ion batteries,  $\text{LiNi}_{0.5}\text{Mn}_{1.5}\text{O}_4$ , HF, alkali carbonate, additive, linear carbonate

# Contents

Abstract .....	i
List of contents .....	ii
List of tables .....	iv
List of figures .....	v

## I. Inorganic electrolyte and electrode additives for 5 V $\text{LiNi}_{0.5}\text{Mn}_{1.5}\text{O}_4$

1. INTRODUCTION .....	1
2. METHODS AND MATERIALS	
2.1. Chemicals .....	1
2.2. Preparation of electrolytes .....	2
2.3. Preparation of electrodes and separator .....	3
2.4. Coin-type cell assembly .....	3
2.5. Electrochemical performance tests .....	4
2.6. Self-discharge test .....	5
2.7. Surface composition analysis of LNMO electrodes .....	5
2.8. Cyclic voltammetry .....	5
3. RESULTS	
3.1 The effect of the electrode additive alkali carbonate on cell performance .....	6
3.2 The effect of the electrolyte additive alkali carbonate on cell performance .....	11
3.3 Surface composition analysis of LNMO electrodes .....	14
3.4 The effect of the electrolyte additive alkali carbonate as an HF scavenger .....	18
4. CONCLUSION .....	18

## II. Linear carbonate effect for 5 V $\text{LiNi}_{0.5}\text{Mn}_{1.5}\text{O}_4$

1. INTRODUCTION .....	20
2. METHODS AND MATERIALS	
2.1. Chemicals .....	22
2.2. Preparation of electrolytes .....	22
2.3. Preparation of electrodes and separator .....	23
2.4. Coin-type cell assembly .....	23
3. RESULTS	
3.1 The effect of the linear carbonates on cell performance .....	23
3.2 The effect of the linear carbonates on self-discharge test .....	27
3.3 Surface composition analysis of LNMO electrodes with linear carbonates .....	28
3.4 $\text{LiNi}_{0.5}\text{Mn}_{1.5}\text{O}_4$ / lithium foil cell EIS test .....	31
4. CONCLUSION .....	32
Reference .....	33



## **List of tables**

Table 1-1. Electrodes of each type of coin cell

Table 1-2. Self-discharge comparison of time to potential

Table 1-3. Initial capacities and coulombic efficiencies of alkali carbonate additive electrolyte compared with the control group

Table 1-4. 100<sup>th</sup> capacities and coulombic efficiencies of alkali carbonate additive electrolyte compared with the control electrolyte

Table 2-1. Physical and chemical properties of solvents

Table 2-2. Self-discharge comparison of time to potential

## **List of figures**

Fig.1-1. Schematic of the degradation mechanism of HF

Fig.1-2. An illustration of the coin-type cell parts and assembly

Fig.1-3. Diagram of three electrodes configuration for cyclic voltammetry

Fig.1-4. First cycle profiles of LNMO / graphite coin full cell with 5 wt. % 25 °C, 5 wt.% 55 °C, 1 wt.% 60 °C, in 1M LiPF<sub>6</sub> in EC / EMC (1/2, v/v).

Fig.1-5. Cycling performances and accumulated efficiency loss of LNMO / graphite full coin cell with 5 wt.% 25 °C, 5 wt.% 55 °C, 1 wt.% 60 °C, in 1M LiPF<sub>6</sub> in EC / EMC (1/2, v/v).

Fig.1-6. Open circuit voltage evolution of four LNMO half cells with a pristine electrode and an electrode containing alkali carbonates (1 wt.%) at the fully charged state.

Fig1. 1-7. First cycle and 100<sup>th</sup> cycle profiles of LNMO / Li metal half cells with pristine and saturated alkali carbonate additive electrolytes in 1M LiPF<sub>6</sub> in EC / EMC (1/2, v/v) at 55 °C.

Fig.1-8. Cycling performance and accumulated efficiency loss of LNMO / Li metal half cells with pristine and saturated alkali carbonate additive electrolytes in 1M LiPF<sub>6</sub> in EC / EMC (1/2, v/v) at 55 °C.

Fig. 1-9. XPS C 1s spectra of the LNMO half cells with pristine electrode and saturated electrolytes containing alkali carbonates after 3 formation cycles

Fig. 1-10. XPS and O 1s spectra of the LNMO half cells with pristine electrode and saturated electrolytes containing alkali carbonates after 3 formation cycles

Fig. 1-11. XPS F 1s spectra of the LNMO half cells with pristine electrodes and saturated electrolytes containing alkali carbonates after 3 formation cycles

Fig. 1-12. Mn 2p spectra of the LNMO half cells with pristine electrode and saturated electrolytes containing alkali carbonates after 3 formation cycles

Fig. 1-13. Cyclic voltammograms of the electrolytes before and after the addition of 500 ppm of HF

Fig. 2-1. Conductivity of 1M LiPF<sub>6</sub>/Ethylene carbonate with a different carbonate at 20 °C

Fig. 2-2. LNMO / Li metal half-cell C-rate performance at each rate and 0.5C cycle performance at 25 °C with linear carbonate

Fig. 2-3. The charge-discharge profiles of LNMO/Li metal half cells with different C-rate and linear carbonate

Fig. 2-4. LNMO / Li metal half-cell performance and accumulated efficiency losses at 55 °C with linear carbonate

Fig. 2-5. LNMO / Graphite full-cell C-rate performance at each rate and 0.5C cycle performance at 25 °C with linear carbonate

Fig. 2-6. LNMO / Graphite full-cell performance and accumulated efficiency losses at 55 °C with linear carbonate

Fig. 2-7. Open circuit of voltage evolution of four LNMO half cells with EC-DMC, EC-EMC, and EC-DEC

Fig. 2-8. XPS C1 s spectra of the LNMO half cells with EC-DMC and EC-DEC after 200 cycle performance at 55 °C

Fig. 2-9. XPS O1 s spectra of LNMO half cells with EC-DMC and EC-DEC after 200 performance cycles at 55 °C

Fig. 2-10. XPS Mn 2 p<sub>3/2</sub> spectra of the LNMO half cells with EC-DMC and EC-DEC after 200 cycle performance at 55 °C

Fig. 2-11. XPS Mn 2 p<sub>3/2</sub> spectra of the LNMO half cells with EC-DMC and EC-DEC after 200 performance cycles at 55 °C

Fig. 2-12. XPS P 2p spectra of the LNMO half cells with EC-DMC and EC-DEC after 200 performance cycles at 55 °C

Fig. 2-13. Electrochemical impedance spectra of LNMO / Li cells in EC-DMC, EC-EMC, and EC-DEC electrolyte after 200 performance cycles tests at 55 °C

Fig. 2-14. The concentration of HF and moisture before and after high temperature storage along with linear carbonates

# I. Inorganic electrolyte and electrode additives for 5 V LiNi<sub>0.5</sub>Mn<sub>1.5</sub>O<sub>4</sub> / graphite cells

## 1. Introduction

There are currently various efforts underway to develop new electrode materials to increase the energy density of lithium ion batteries for electric vehicles (EVs)[1]. LiNi<sub>0.5</sub>Mn<sub>1.5</sub>O<sub>4</sub> (LNMO) is a promising cathode material for lithium-ion batteries due to its low cost, being non-toxic, and its high operation voltage capacity for high energy demands, such as electric vehicles[2-6]. However, LNMO suffers from severe electrolyte decomposition and a manganese dissolution issue at high voltage and manganese dissolution and the destruction of the solid electrolyte interphase (SEI) by hydrofluoric acid (HF), which contributes greatly to the degradation of LNMO/ graphite cells. Specifically, the destruction of the SEI layer by HF can contribute to electrolyte decomposition by forming an additional SEI layer formation. Hydrofluoric acid (HF) is formed from LiPF<sub>6</sub> salt with H<sub>2</sub>O via the following equation.

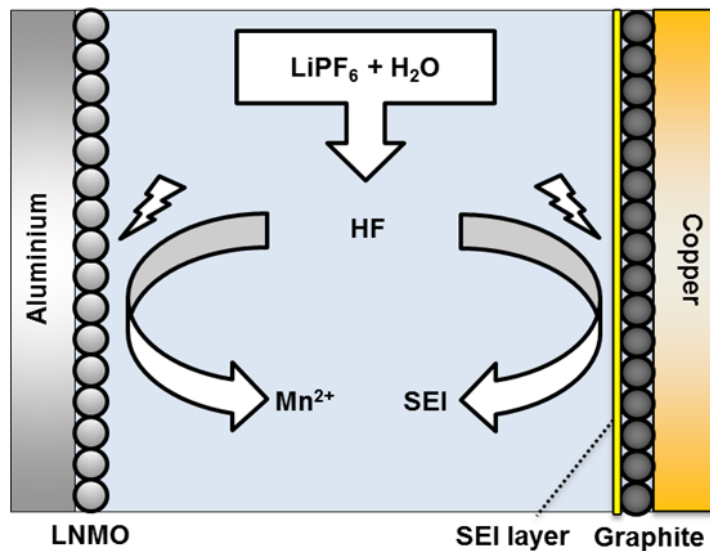
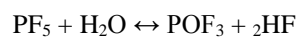
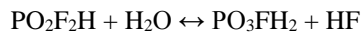


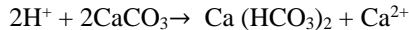
Fig. 1. Schematic of degradation mechanism by HF





Hydrofluoric acid also forms the lithium fluoride (LiF) layer which hampers later formation and increases resistance on the cathode and anode surfaces. So far, extensive studies have been devoted to suppress HF formation, and thus various additives have been used.

So far, alkali carbonates such as  $\text{Li}_2\text{CO}_3$ ,  $\text{Na}_2\text{CO}_3$  and  $\text{CaCO}_3$  have been examined as additives to improve anode performance[7-11], and  $\text{Li}_2\text{CO}_3$  have been also used electrolyte additive to enhance cathode performance[12]. It has been shown that the alkali carbonate additives exhibited a significant effect on modifying the SEI formation during the first charge process and that these additives successfully suppress the initial irreversibility and improve graphite cycle performance as the electrolyte additive[13]. Also, alkali carbonate has been confirmed as an HF scavenger in lithium ion batteries, as has been previously reported[14]. It exhibits improved cycling performance because the alkaline  $\text{CaCO}_3$  neutralizes the acidic products. The  $\text{CaCO}_3$  additive neutralizes the formed acids via this reaction:[15]



Herein, alkali carbonate additives were used as additives in the electrolyte and electrode to improve cycling performance and the efficiency of  $\text{LiNi}_{0.5}\text{Mn}_{1.5}\text{O}_4$  (LNMO) by HF scavenging effect. To confirm the effect of alkali carbonates through coin-type cell, additives were saturated in electrolyte and added 1 wt.% and 5 wt.% to the electrode. These additives successfully improved cycle performance and the self-discharge of LNMO at a high temperature of 55°C.

## 2. Methods and materials

### 2.1 Chemicals

Calcium carbonate (99.999%), magnesium carbonate (99.5%), and lithium carbonate (99.99%) were purchased from Aldrich. Battery grade 1M  $\text{LiPF}_6$  in ethylene carbonate (EC) / ethyl methyl carbonate (EMC) (1/2, v/v) were purchased from Panaxetec and used as the base electrolyte solution.

## 2.2 Preparation of the electrolyte

For pre-treatment, alkali carbonates ( $\text{CaCO}_3$ ,  $\text{MgCO}_3$ ,  $\text{Li}_2\text{CO}_3$ ) were dried in a vacuum for a week at  $110^\circ\text{C}$ . Electrolyte preparation was completed in an Ar-filled glove box. The dried alkali carbonates were added into pure EC / EMC (1/2, v/v) and stirred for a week. Moisture in the electrolyte was removed by molecular sieve, then lithium hexafluorophosphate ( $\text{LiPF}_6$ , Panaxetec Co., Korea) was added to make 1M  $\text{LiPF}_6$  in EC / EMC (1/2, v/v). 1M  $\text{LiPF}_6$  in EC / EMC (1/2, v/v) was used as the base electrolyte, and each additive ( $\text{CaCO}_3$ ,  $\text{MgCO}_3$ ,  $\text{Li}_2\text{CO}_3$ ) was saturated in 1M  $\text{LiPF}_6$  in EC / EMC (1/2, v/v).

## 2.3 Preparation of the electrode and separator

Alkali carbonates were added to the base electrode ( $\text{LiNi}_{0.5}\text{Mn}_{1.5}\text{O}_4$  : PVDF : Super-P = 90 : 5 : 5,  $1.17\text{mAh/cm}^2$ ). For the preparation of electrodes with additives,  $\text{LiNi}_{0.5}\text{Mn}_{1.5}\text{O}_4$  (90 wt.%) were mixed with polyvinylidene fluoride (5 wt.%, PVDF) and conductive carbon (5 wt.%, Super. P), in N-methyl pyrrolidinone (NMP) to make the slurry for electrode preparation. 1 wt.% and 5 wt.% of alkali carbonate additives were added to the slurry. The mixtures thus obtained were coated onto aluminum foil and dried at  $110^\circ\text{C}$  in a vacuum prior to use. The electrodes were cut into pieces 14mm in diameter, and these were dried at  $110^\circ\text{C}$  in a vacuum state at least 24 hours prior to use. Poly ethylene separators (Tonen) were punched in 18 mm diameter disks and stored in a glove box.

## 2.4 Coin-type cell assembly

Coin-type cells are widely recognized as the standard test platform for lithium ion battery electrode research. A coin-type cell (diameter, 20 mm; thickness, 3.2 mm) which consisted of  $\text{LiNi}_{0.5}\text{Mn}_{1.5}\text{O}_4$ , a separator, graphite and each electrolyte were assembled in an Ar-filled glove box. In order from the bottom of Fig 2, 150  $\mu\text{l}$  of electrolytes were injected on the bottom of the case. After the electrode was

put in place, a separator and a gasket were installed. An anode was inserted on the gasket with a spacer disk and wave spring. Lastly, the coin-type cell was sealed using a clamping machine. After coin-type cell assembly, wetting was initiated for 20 hours at 25 °C.

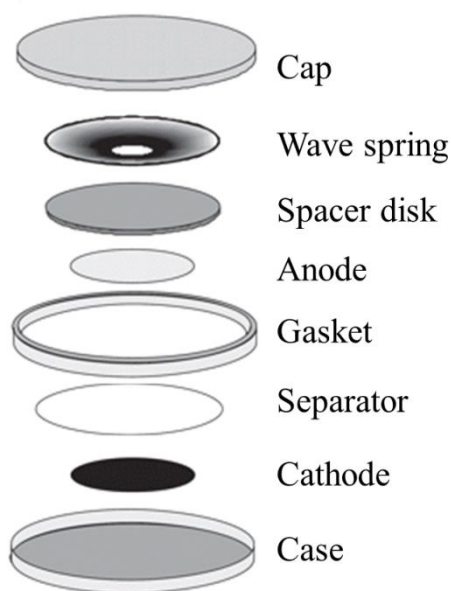


**Fig. 2. An illustration of the coin-type cell parts and assembly**

Electrode	Half cell	Full cell
Cathode	$\text{LiNi}_{0.5}\text{Mn}_{1.5}\text{O}_4$	$\text{LiNi}_{0.5}\text{Mn}_{1.5}\text{O}_4$
Anode	Li metal	Graphite

**Table1. Electrodes of each type of coin cell**

## 2.5 Electrochemical performance tests

To evaluate the effects of the additives ( $\text{CaCO}_3$ ,  $\text{MgCO}_3$ ,  $\text{Li}_2\text{CO}_3$ ), half and full cell tests were performed at 25 °C and 60 °C as well. All the cells were cycled initially at 25 °C over a 3.0~4.8 V range three times with a 0.2C charging current followed by a 4.8 V constant voltage charge (CC/CV) and 0.2C



constant current (CC) discharging to complete the formation process. Cycle tests were performed with 0.5C (CC/CV) and 0.5C (CC) over 3.0~4.8 V at 25 °C, 55 °C and, 60 °C .

## **2.6 Self-discharge test**

Self-discharge studies with coin half-cells were performed after three formation cycles at a 0.2C charge to a cut-off of 4.95V applying 0.2C and a subsequent CV step to 0.05C at a room temperature of 25 °C. Then the cells were moved at 60 °C under an open circuit voltage (OCV) condition for 30 days.

## **2.7 Surface composition analysis of LNMO electrodes**

To investigate the mechanism of alkali carbonate additives for improved high temperature performances, the surface of the electrode after electrochemical cycling was observed with scanning electron microscopy (SEM) and X-ray photoelectron spectroscopy (XPS). To prepare SEM and XPS measurements, each of the electrodes were cycled three times at 0.2C, then the electrodes were washed with pure EMC to remove the precipitates on the electrode surface prior to SEM and XPS, and vacuum dried overnight at 60 °C.

## **2.8 Cyclic voltammetry**

Cyclic voltammetry analysis was used to certify the HF scavenging effect of alkali carbonate additives. All of the cyclic voltammetry tests were performed in an Ar-atmosphere glove box at 25 °C. A three electrodes configuration was employed for cyclic voltammetry. The reference electrode was Li metal foil and the working electrode was a Pt plane (area=0.02 cm<sup>2</sup>) electrode. The Pt wire electrode was used as the counter electrode. The scan rate was fixed as 10 mV/s. Cyclic voltammetry tests were operated in the

potential range between 4.2 and 0V (vs. Li/Li<sup>+</sup>). The working and counter electrodes were polished with alumina powder and sand paper to remove foreign materials before cyclic voltammetry.

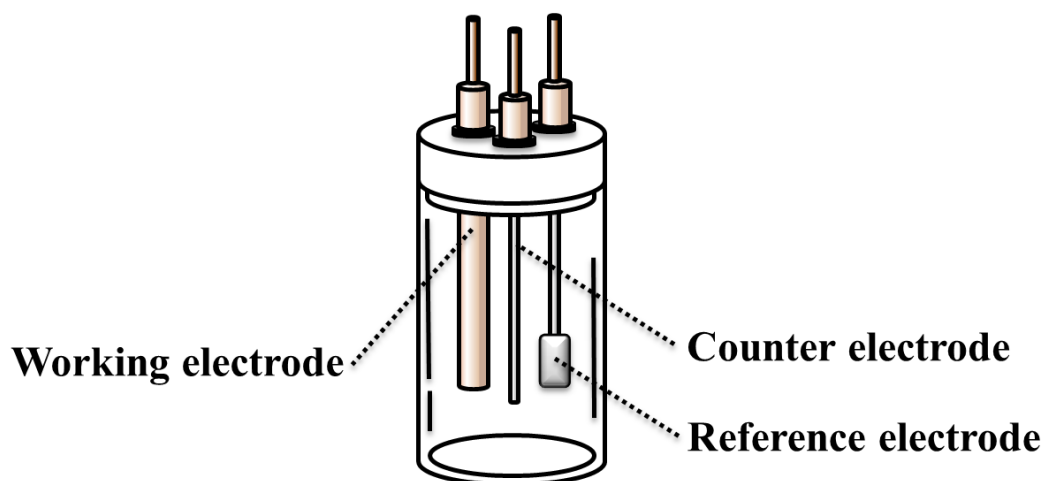


**Fig. 3. Diagram of the three electrodes configuration for cyclic voltammetry**

### **3. Result**

#### **3.1 The effect of the electrode additive alkali carbonate on cell performance**

To investigate the effects of alkali carbonate on LiNi<sub>0.5</sub>Mn<sub>1.5</sub>O<sub>4</sub> performance, full cells were assembled with each LNMO cathode containing 1 wt.%, and 5 wt.% of alkali carbonate electrode additives. All coin-type cells were cycled at a room temperature of 25 degrees Celsius to make a stable and homogeneous solid electrolyte interface (SEI) layer on the electrode's surface. Fig.4 shows the initial charge and discharge curves of LNMO/Graphite cells. Their capacities, efficiencies, and amount of additives are summarized with comparisons in each table. The coulombic efficiency was defined as (discharge capacity) / (charge capacity)\*100% at the first cycle. The pristine LNMO exhibited 147.06 mAh/g<sup>-1</sup> of an average charge capacity with an average coulombic efficiency of 86.2%. In the case of LNMOs containing CaCO<sub>3</sub>,

MgCO<sub>3</sub> and Li<sub>2</sub>CO<sub>3</sub>, average charge capacities of 144.5, 141.1, 142.4 mAh/g<sup>-1</sup> and average coulombic efficiencies of 85.5, 85.9, 86.6%, were shown respectively. The pristine LNMO exhibited the highest value among the specific capacities. Additionally, the coulombic efficiency did not vary.

Fig.5 depicts the specific capacity for the 100 charge-discharge cycles, and accumulated efficiency loss ( $S_n$ ). The “efficiency loss” was defined as: 100% minus the shown efficiency values[16]. Over the discharge/charge cycle numbers, the loss of efficiency was increased as demonstrated in Fig.5. Loss of all cycles were integrated to get an accumulated efficiency loss, as defined by the following equation (1)

$$S_{n=0} = 0$$

$$S_n = S_{n-1} + \left(1 - \frac{C_{Dis}}{C_{chg}}\right) \cdot 100 \quad (1)$$

As shown in Fig.5, pristine LNMO shows the slowest fading capacity and accumulated efficiency loss in the case of the 5 wt.% additives at room temperature. However, in the case of the Li<sub>2</sub>CO<sub>3</sub> additive, the fading rate of capacity was improved at the higher temperature of 55 degrees Celsius and efficiency was also similar with pristine LNMO. This clearly demonstrates that the 60°C cyclability of LNMO cells are greatly improved by alkali carbonate additives in the following order: CaCO<sub>3</sub>  $\approx$  Li<sub>2</sub>CO<sub>3</sub>  $\geq$  MgCO<sub>3</sub> base.

Self-discharge studies with coin half-cells were performed in the following conditions: At room temperature, three formation cycles at 0.2C charges, to a cut-off potential of 4.95 V applying 0.2C and a subsequent CV step to 0.05C. Then the cells were moved at 60°C under OCV conditions for 900 h while the potential of the cells was recorded. As shown in Fig. 6, the potential of every cell decreased rapidly to 4.73 V.

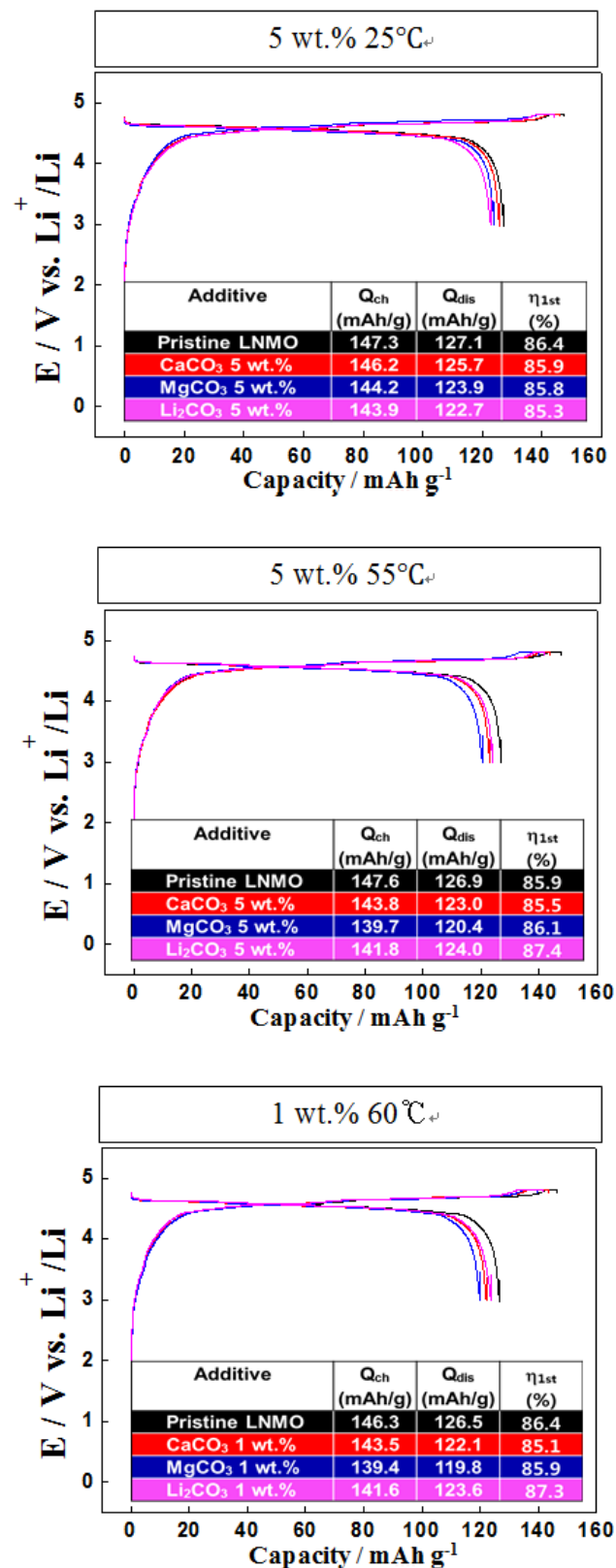


Fig. 4. First cycle profiles of LNMO / graphite full coin cell with 5 wt.% 25°C, 5 wt.% 55°C, 1 wt.% 60 °C, in 1M LiPF<sub>6</sub> in EC / EMC (1/2, v/v).

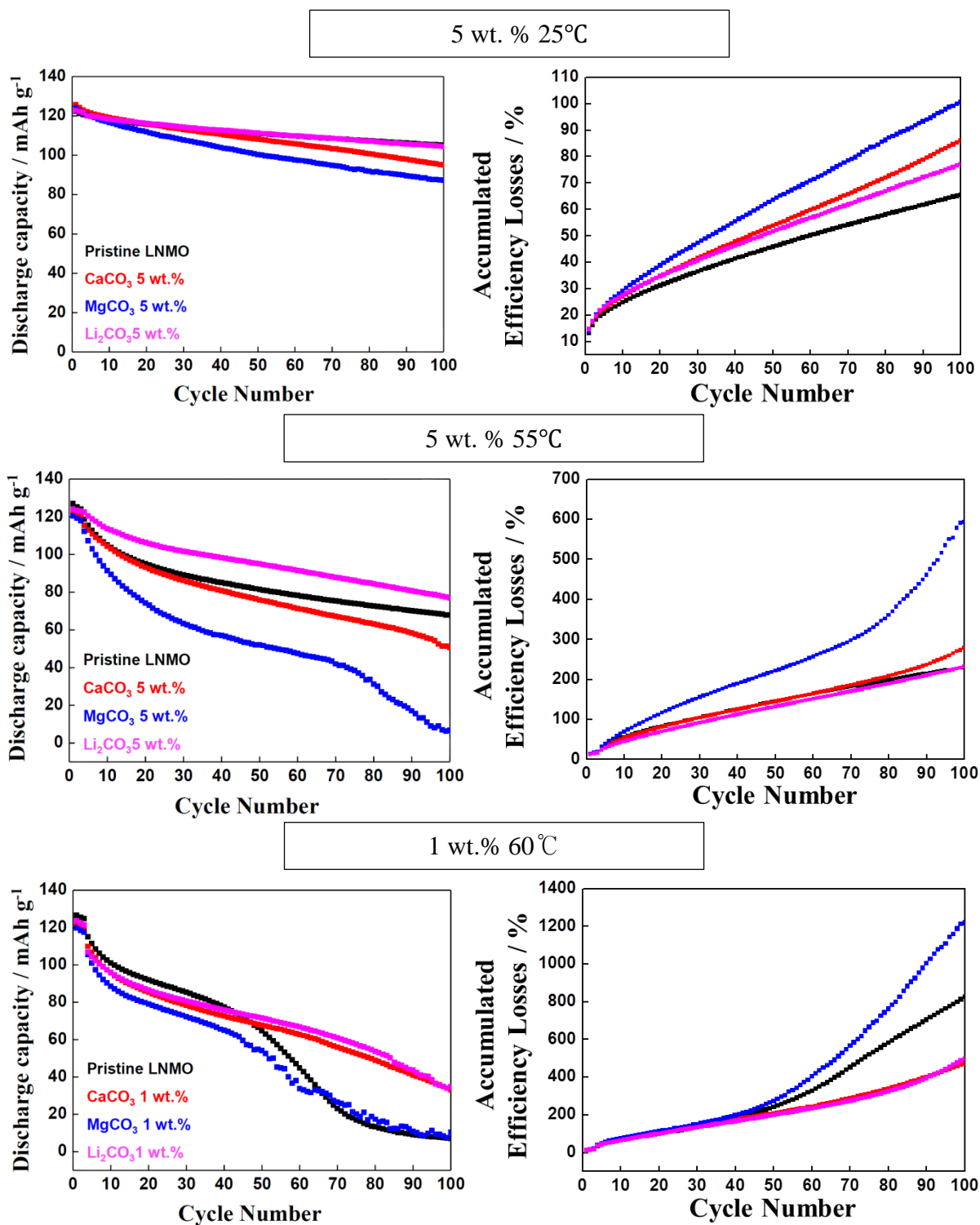


Fig. 5. Cycling performances and accumulated efficiency loss of LNMO / graphite full coin cell with 5 wt. %

25 °C, 5 wt.% 55 °C, 1 wt.% 60 °C, in 1M LiPF<sub>6</sub> in EC / EMC (1/2, v/v).

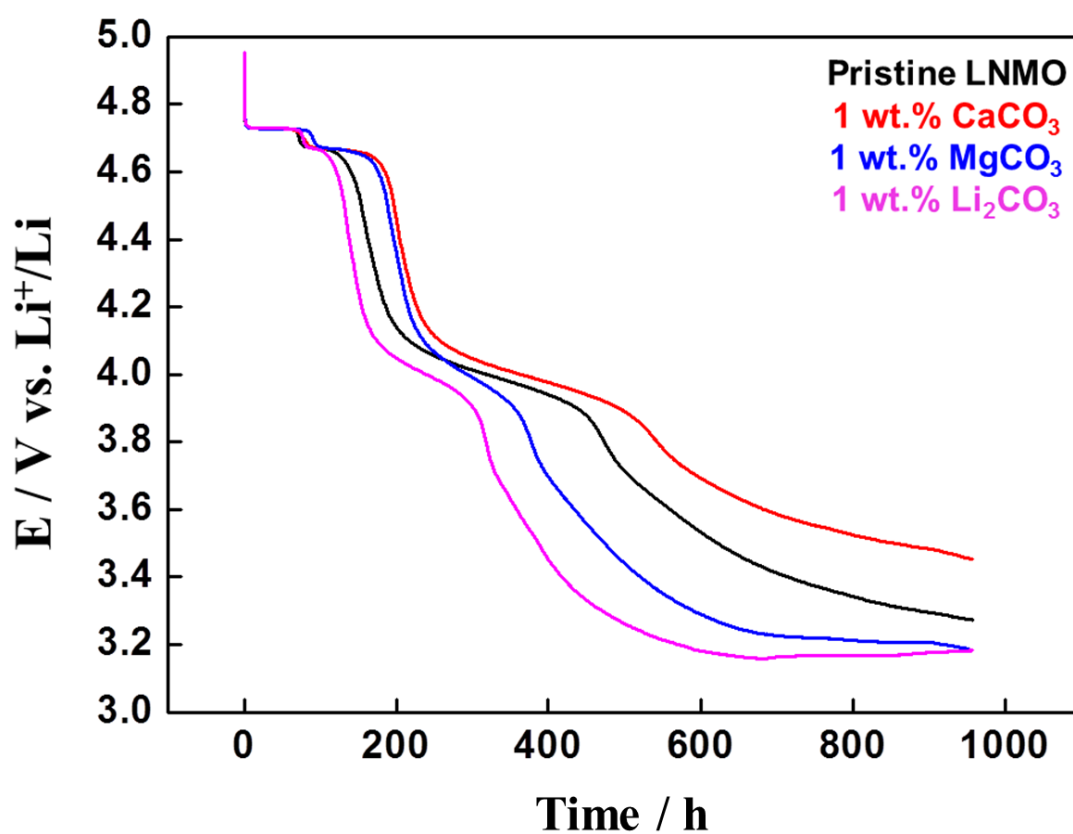


Fig. 6. Open circuit of voltage evolution of four LNMO half cells with a pristine electrode and an electrode containing alkali carbonates (1 wt.%) at the fully charged state.

	Reference	CaCO <sub>3</sub>	MgCO <sub>3</sub>	Li <sub>2</sub> CO <sub>3</sub>
Time to 3.6V (Self-discharge)	550h	700h	430h	350h
Potential at 900hours	3.29V	3.47V	3.2V	3.2V

Table 2. Self-discharge comparison of time to potential

However, in the case of the CaCO<sub>3</sub> electrolyte additive, a better performance was observed compared

with pristine LNMO. Specifically, the time of the voltage drop to 3.6V was 150 hours longer than pristine LNMO. After self-discharging for 900 hours, potentials were clearly shown in the following order:  $\text{CaCO}_3$  (3.47 V) > Reference (3.29 V) >  $\text{MgCO}_3 \approx \text{Li}_2\text{CO}_3$  (3.2 V). This clearly demonstrates that  $\text{CaCO}_3$  takes the role of an HF scavenger, which prevents HF formation from  $\text{H}_2\text{O}$  and  $\text{LiPF}_6$ . However, other cases exhibit lower performances in terms of self-discharge.

### **3. 2 The effect of the electrolyte additive alkali carbonate on cell performance**

To confirm the electrolyte additive effects with alkali carbonate on LNMO performance, the electrolytes were used with each additive ( $\text{CaCO}_3$ ,  $\text{MgCO}_3$ ,  $\text{Li}_2\text{CO}_3$ ) saturated in 1M  $\text{LiPF}_6$  in EC / EMC (1/2, v/v). The performances of LNMO / Li metal half cells were evaluated at 55 °C.

Fig.7 indicates the initial and 100<sup>th</sup> charge-discharge profiles of LNMO/Li metal cells. Each charge capacity, discharge capacity and coulombic efficiencies are summarized in tables 2 and 3. As shown in Table 3, the reference and  $\text{CaCO}_3$  electrolyte additives showed very similar charge-discharge capacities and efficiencies. In the case of  $\text{MgCO}_3$  and  $\text{Li}_2\text{CO}_3$  electrolyte additives, initial charge-discharge capacities were less than those without additives, but the reference electrolyte clearly showed a faster fading rate. Fig. 7 shows the over-potential differences between reference and additive conditions. In the case of the first cycle profile, all cells show similar charge-discharge behavior. However, the ohmic over-potential of those without additives clearly increased more than  $\text{CaCO}_3$  and  $\text{MgCO}_3$  added electrolyte after 100 cycles at 55 °C. This factor contributes to the decomposition characteristic of the electrolyte. It means smaller polarization is generated and enhanced reversibility of the cathode occurs in the presence of  $\text{CaCO}_3$  and  $\text{MgCO}_3$ .

	Reference	CaCO <sub>3</sub>	MgCO <sub>3</sub>	Li <sub>2</sub> CO <sub>3</sub>
Charge( mAh/g )	142.5	142.9	139.2	139.2
Discharge( mAh/g )	137.5	137.8	134.5	133.9
Efficiency (%)	96.4	96.4	96.6	96.1

**Table 3. Initial capacities and coulombic efficiencies of alkali carbonate additive electrolytes compared with the control group**

	Reference	CaCO <sub>3</sub>	MgCO <sub>3</sub>	Li <sub>2</sub> CO <sub>3</sub>
Charge( mAh/g )	85.5	118.4	123.0	90.1
Discharge( mAh/g )	82.5	113.4	118.9	85.6
Efficiency (%)	96.5	95.7	96.6	95.0

**Table 4. 100<sup>th</sup> capacities and coulombic efficiencies of alkali carbonate additive electrolytes compared with the control electrolyte**

Fig. 8 depicts the cycling performance and accumulated efficiency loss at 55 °C. It shows that the 55 °C cycle performance of LNMO/Li half cells greatly improved, including the alkali carbonate electrolyte. In particular, CaCO<sub>3</sub> was observed to exhibit the highest capacity retention of about 74.8% compared with MgCO<sub>3</sub> (about 74.8%) and Li<sub>2</sub>CO<sub>3</sub> (about 47.6%) after 120 cycles. However, the reference electrolyte capacity retention is only 19.0%.



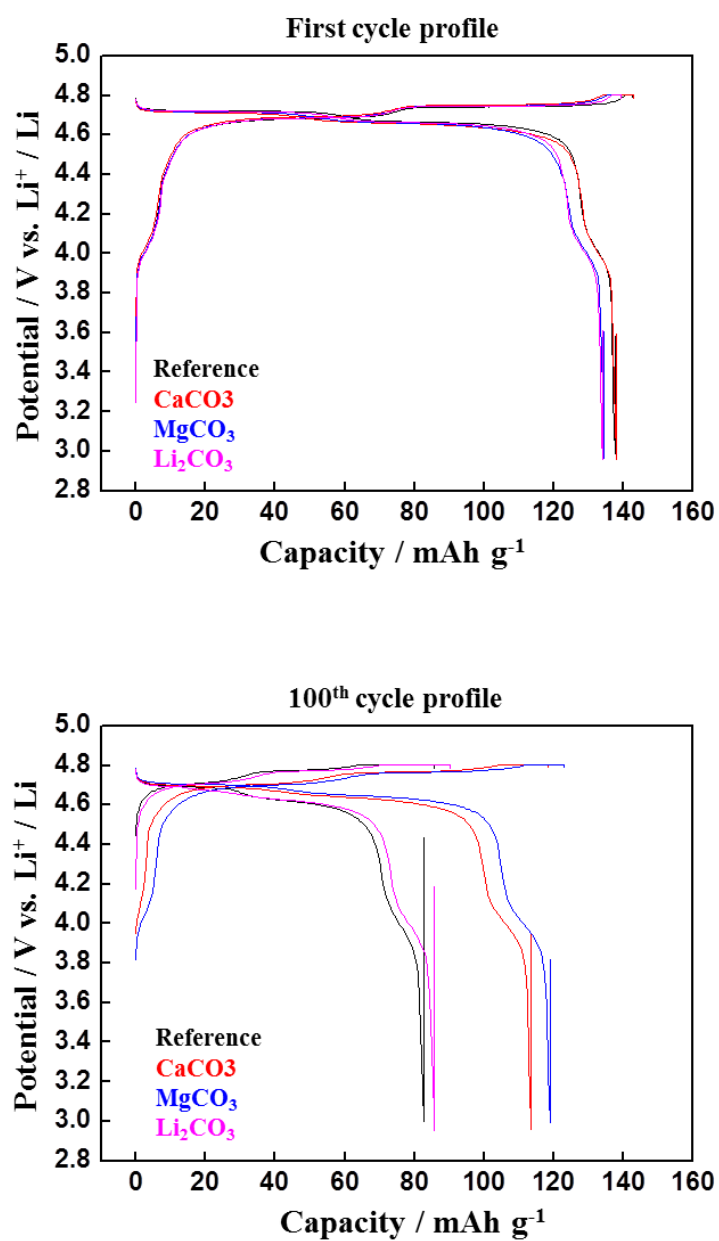


**Fig. 7.** First cycle and 100<sup>th</sup> cycle profiles of LNMO / Li metal half cells with pristine and saturated alkali carbonate additive electrolytes in 1M LiPF<sub>6</sub> in EC / EMC (1/2, v/v) at 55 °C.

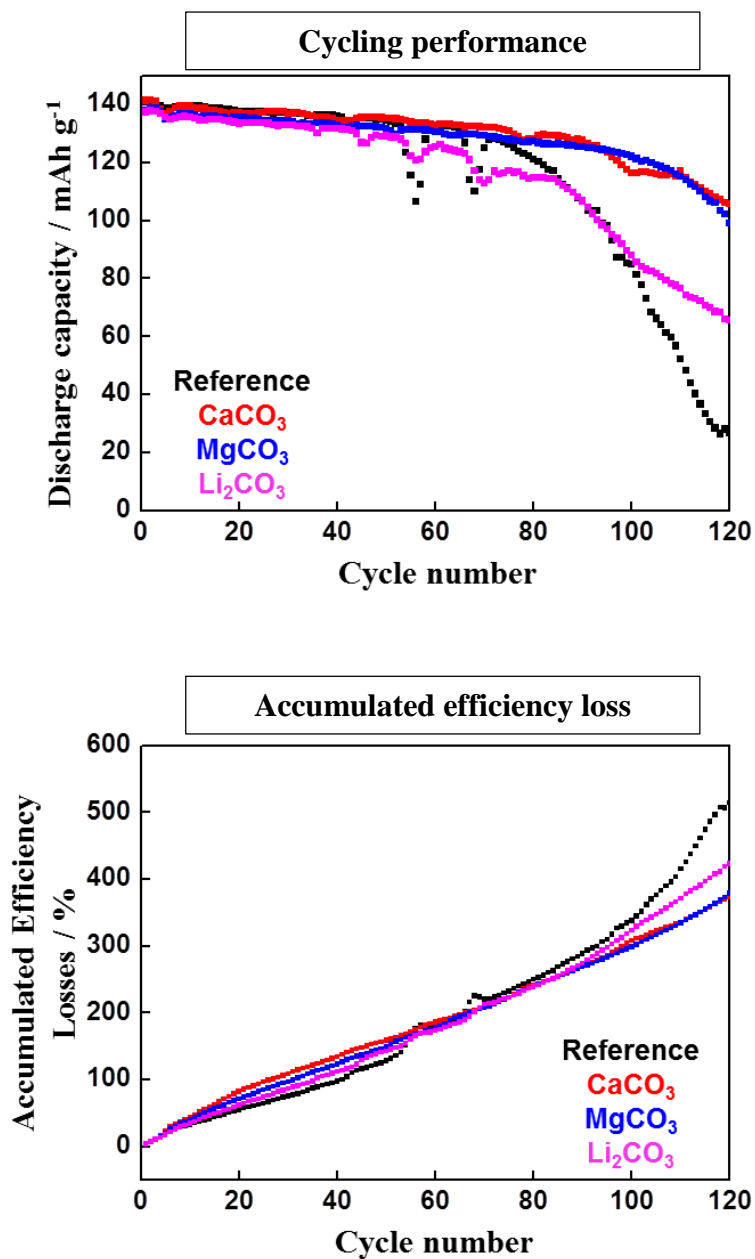


Fig. 8. Cycling performance and accumulated efficiency loss of LNMO / Li metal half cells with pristine and saturated alkali carbonate additive electrolytes in 1M LiPF<sub>6</sub> in EC / EMC (1/2, v/v) at 55 °C.

### 3.3 Surface composition analysis of LNMO electrodes

To investigate the mechanism of alkali carbonate additives for improved cycling performance at 55 °C

and self-discharge, X-ray photoelectron spectroscopy (XPS) analysis was carried out. To XPS analysis, LNMO electrodes went through the formation cycle with and without the addition of alkali carbonates, respectively.

The C 1s spectra include peaks of C-F (291.2 eV)[17], C=O (289.4 eV), C-O (286.5 eV), C-H (285.3 eV), and C-C (284. eV), standing for the PVDF, substances of carbonate ( $\text{CO}_3^{2-}$ ), metal oxide, lithium alkoxide (R-OLi)[18], and conductive carbon. This clearly demonstrates that the electrolytes including alkali carbonate additives suppress the decomposition of the electrolyte from the result of C-C peak intensities.

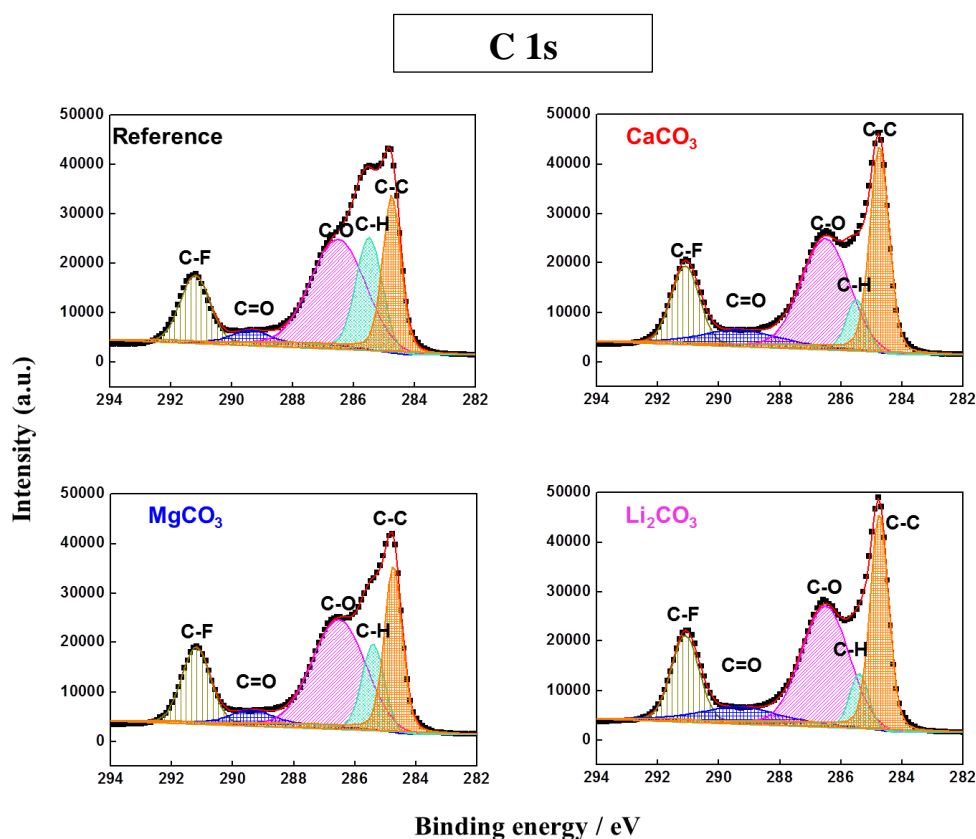


**Fig. 9. XPS C1 s spectra of the LNMO half cells with pristine electrode and saturated electrolytes containing alkali carbonates after 3 formation cycles**

And, the O 1s spectra show peaks C-O (533.7 eV), C=O (532.5 eV), and M-O (530.0 eV) which means lithium alkoxide (R-OLi), substances of carbonate ( $\text{CO}_3^{2-}$ ), and metal oxide are present[19]. The intensities

of the M-O peak increase in the following order:  $\text{Li}_2\text{CO}_3 \geq \text{CaCO}_3 > \text{MgCO}_3 > \text{base}$ . This indicates that a lower content of oxidation occurs on the cathode surface with alkali carbonate additives.

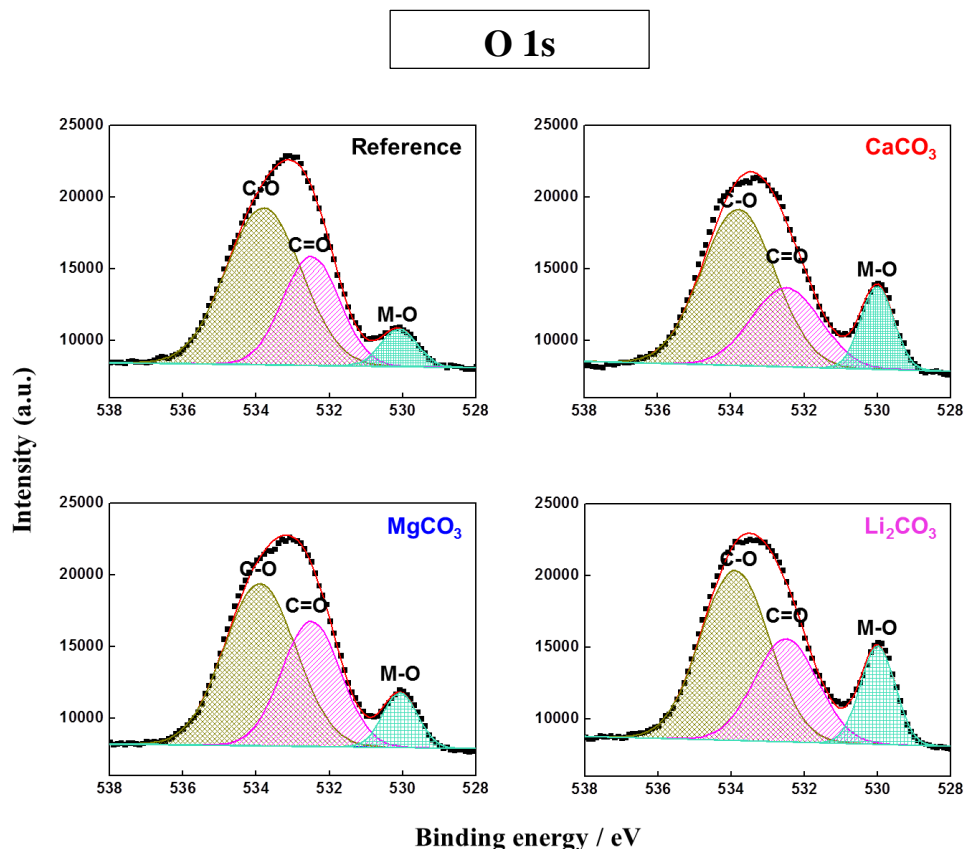


**Fig. 10. XPS and O 1s spectra of the LNMO half cells with pristine electrode and saturated electrolytes containing alkali carbonates after 3 formation cycles**

The peak of LiF (685.5 eV) that increases resistance on the active material is relatively lower with alkali carbonates. This result means that the decomposition of  $\text{LiPF}_6$  producing LiF is weakened by adding alkali carbonates. Also, the C-F peak (688.3 eV) means that the PVDF is higher compared with the reference electrolyte. This is attributed to the fact that the LNMO surface was covered by electrolyte decomposition products. So, a smaller C-F peak with the reference electrolyte was confirmed. The Mn 2p spectra contains a peak of Mn-O (655 eV and 642.5 eV)[20]. The intensity of the Mn-O peak with electrolyte additives clearly implies suppression of manganese dissolution and a thinner SEI.

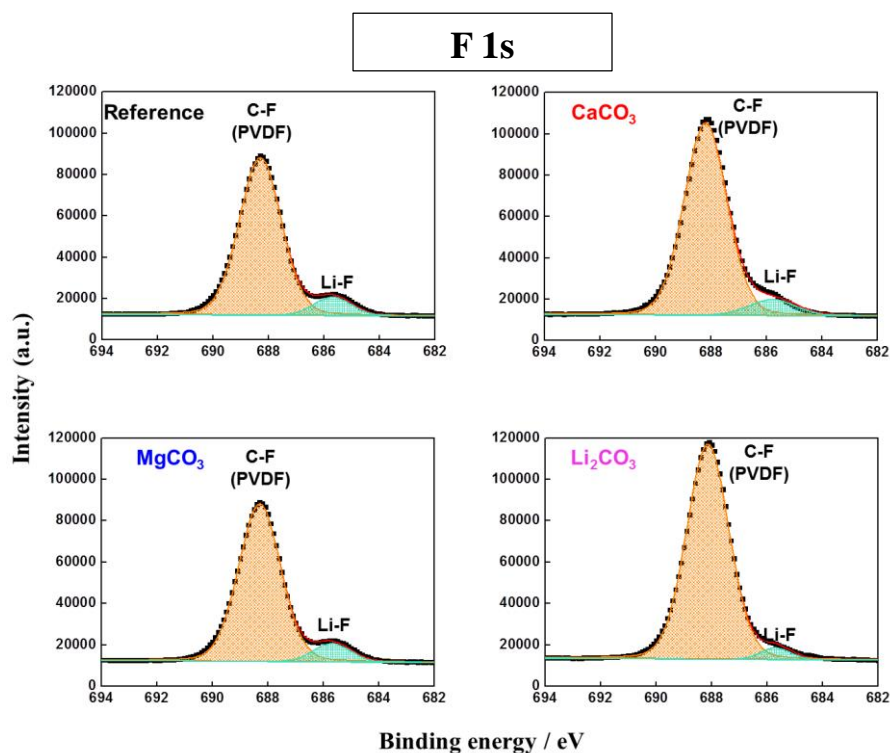


Fig. 11. XPS F 1s spectra of the LNMO half cells with pristine electrode and saturated electrolytes containing alkali carbonates after 3 formation cycles

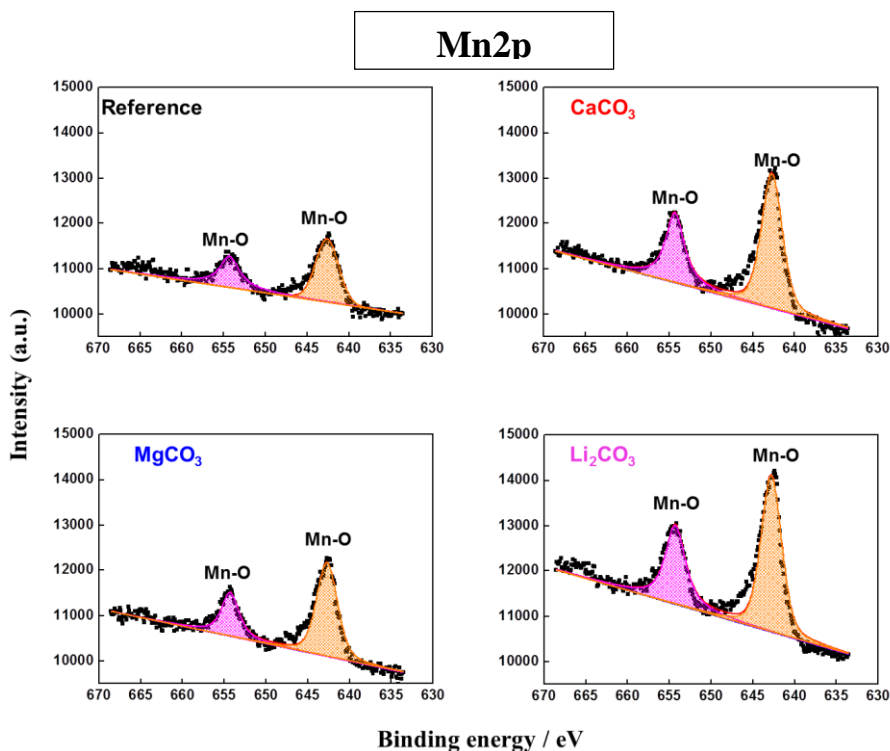


Fig. 12. Mn 2p spectra of the LNMO half cells with pristine electrode and saturated electrolytes containing alkali carbonates after 3 formation cycles

### 3.4 The effect of the electrolyte additive alkali carbonate as an HF scavenger

To investigate the HF scavenging effect of alkali carbonate additives in the electrolyte, cyclic voltammetry analysis was performed. The 500 ppm of HF solution was added in the electrolytes with and without alkali carbonate additives. These solutions were stored in an Ar-atmosphere glove box for 7 days. The electrolytes before the addition of HF show almost the same reduction peaks of current density which occurred over 2.5~2.2V (vs. Li/Li<sup>+</sup>)[21]. However, the reduction peak differences of current density clearly increased after 500 ppm of HF solution. The electrolytes with added MgCO<sub>3</sub> and CaCO<sub>3</sub> effectively scavenge HF by a neutralization reaction, then the peak intensities are scavenged, which means that HF concentrations decrease more than the reference electrolytes. This result is well in accordance with half-cell performance test results.

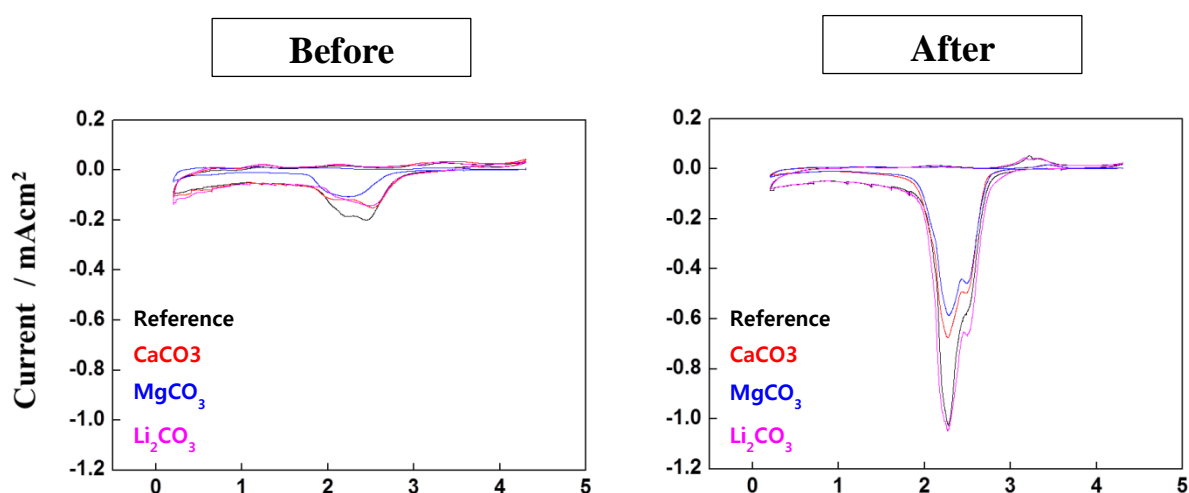


Fig. 13. Cyclic voltammograms of the electrolytes before and after the addition of 500 ppm of HF

## 4. Conclusion

In this study, alkali carbonates including CaCO<sub>3</sub>, MgCO<sub>3</sub>, and Li<sub>2</sub>CO<sub>3</sub> were employed as an electrolyte and electrode additives. The electrochemical performances of LNMO are greatly improved by adding

alkali carbonates as electrolyte and electrode additives. From the electrochemical tests, It is revealed that  $\text{CaCO}_3$  as an electrode and electrolyte additive greatly improves the cycle performances at 25 °C and 55 °C and self-discharge behavior at 60 °C. It contributes to a kinetic enhancement through the inhibition of a side reaction of an HF scavenging effect, which was verified by cyclic voltammetry (CV) and XPS. In the case of the alkali carbonate-free condition, it increases IR resistance because the surfaces of the cathode were accumulated by the electrolyte's decomposition product, which was confirmed using XPS as well as the charge-discharge profile.

## II. Linear carbonate effect for 5 V LiNi<sub>0.5</sub>Mn<sub>1.5</sub>O<sub>4</sub>

### 1. Introduction

Rechargeable lithium (Li) ion batteries have been widely used in such portable electronics as VCRs, cellular phones and laptop PCs. Further, advanced battery systems with higher performance abilities are now required for power sources of energy storage and electric vehicle (EV) applications. For those purposes, lithium ion batteries have displayed a higher energy and power density and thermal stability than other battery types. [22] As a result, many researches have been examining how to improve lithium ion batteries with variations of electrolyte composition. The electrolytes in lithium ion batteries were divided into cyclic and linear carbonates. The cyclic carbonates such as propylene carbonate and ethylene carbonate (EC) have a high di-electric constant, viscosity, and surface energy. But the linear carbonates have low di-electricity, viscosity, and surface energy. The cyclic carbonates can easily dissolve inorganic Li salts (LiPF<sub>6</sub>, LiBF<sub>4</sub>, etc.) but these cyclic carbonates exhibit low ionic conductivity compared with linear carbonates because of high viscosity. So, the linear and cyclic carbonates in lithium ion batteries were generally mixed to increase ionic conductivity and the solubility of inorganic Li salts.

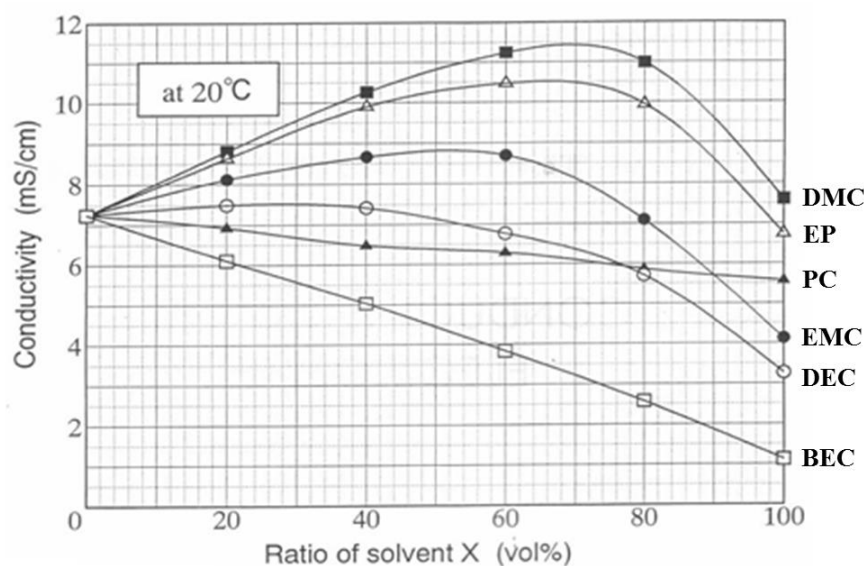


Fig. 1. Conductivity of 1M LiPF<sub>6</sub>/Ethylene carbonate with a different carbonate at 20 °C



Fig.1 shows the conductivities of ethylene carbonate with a co-solvent. The major factor determining the conductivity of an electrolyte is the viscosity of the electrolyte. [23] The 1M LiPF<sub>6</sub> in ethylene carbonate (EC) / dimethyl carbonate (DMC) (3/7, v/v) exhibits high conductivity compared with ethyl methyl carbonate and diethyl carbonate. This is mainly due to the dielectric constant and viscosity of linear carbonates.

	Propylene carbonate (PC)	Ethylene carbonate (EC)	Dimethyl carbonate (DMC)	Ethylmethyl carbonate (EMC)	Diethyl carbonate (DEC)
Molecular weight	102.09	88.09	90.08	104.11	118.13
Boiling point (°C)	242	244	90	107	126
Melting point (°C)	-49	39	0.5	-55	-74
Density	1.21	1.32	1.07	1.007	0.975
Dielectric constant	65	90	3.1	2.8	2.8
Viscosity (cP)	2.53	1.92	0.625	0.665	0.736
HOMO energy (eV)	-7.63	-7.70	-7.80	-7.30	-7.25

**Table1. Physical and chemical properties of solvents**

The choice of co-solvent is an important issue because it greatly affects not only the conductivity, but also performance, such as capacities and efficiencies. [24] Many research groups have reported

electrochemical behavior of organic electrolyte solution based on carbonate with different compositions. [25-29] For example, EC-DMC composition exhibits better cycle performance than EC-EMC and EC-DEC composition for 5 V Li-ion batteries in the paper of Wu et al. [30] However, the paper of Julien Demeaux [31] insists that EC-EMC has better performance than EC-DMC in case of self-discharge test. This result implies that DMC composition promotes severe transition metal dissolution because of low activation energy.

The purpose of this study is to compare and interpret the electrochemical performances with linear carbonates for  $\text{LiNi}_{0.5}\text{Mn}_{1.5}\text{O}_4$  (LNMO). To confirm the difference of performance with linear carbonates, coin-type cell tests were carried out at 25 °C and 55 °C and then a surface analysis was performed after coin-type cell tests to investigate the effect of linear carbonates.

## **2. Methods and materials**

### **2.1 Chemicals**

Battery grade ethylene carbonate (EC), diethyl carbonate (EMC), dimethyl carbonate (DMC), and ethyl methyl carbonate (EMC) were obtained from Panaxetec Co. in Korea. All electrolytes were dried with molecular sieves in an Ar-filled glove box. Linear carbonates (DMC, DEC, EMC) were mixed with EC (EC:LC ratio : 3/7, v/v).  $\text{LiPF}_6$  was added to the above solution to achieve a concentration of 1.0M, and then the solution was stirred to homogeneity.

### **2.2 Preparation of electrolytes**

Linear carbonates (DMC, DEC, EMC) were mixed with EC (EC:LC ratio : 3/7, v/v). Lithium hexafluorophosphate ( $\text{LiPF}_6$ , Panaxetec Co., Korea) was added to the above solution to achieve a concentration of 1.0M, and then the solution was stirred to homogeneity.

## **2.3 Preparation of electrode and separator**

The  $\text{LiNi}_{0.5}\text{Mn}_{1.5}\text{O}_4$  (LNMO) was used as the base electrode ( $\text{LiNi}_{0.5}\text{Mn}_{1.5}\text{O}_4$ : PVDF : Super-P = 90 : 5 : 5, 1.17 mAh/cm<sup>2</sup>) and dried at 110 °C in a vacuum state at least 24 hours prior to use. The electrodes were cut into pieces 14mm in diameter, and these were dried at 110°C in a vacuum state at least 24 hours prior to use. Poly ethylene separators (Tonen) were punched in 18mm diameter disks and stored in a glove box.

## **2.4 Coin-type cell assembly**

Coin-type cells are widely recognized as the standard test platform for lithium ion battery electrode research. A coin-type cell (diameter, 20 mm; thickness, 3.2 mm) which consisted of  $\text{LiNi}_{0.5}\text{Mn}_{1.5}\text{O}_4$ , a separator, graphite and each electrolyte were assembled in an Ar-filled glove box.

# **3. Result**

## **3.1The effect of the linear carbonates on cell performance**

To evaluate the effects of the linear carbonate (DMC, DEC, EMC), half and full cell tests were performed at a room temperature (25 °C) and at a high temperature of (60 °C) as well. All the cells were cycled initially at 25°C over a 3.0~4.8 V range three times with a 0.2C charging current followed by a 4.8V constant voltage charge (CC/CV) and 0.2C constant current (CC) discharging to complete the formation process. Cycle tests were performed with 0.5C CC/CV and 0.5C CC over 3.0~4.8 V at 25 °C, and 55 °C .

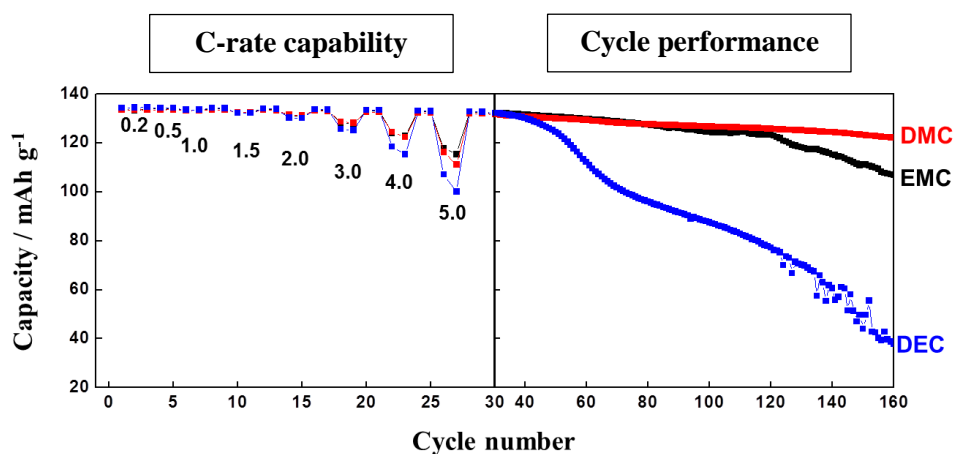


**Fig. 2. LNMO / Li metal half-cell C-rate performance at each rate and 0.5 C cycle performance at 25 °C with linear carbonates**

Fig. 2 presents the C-rate capability and cycle performances of the LNMO / Li metal cells in each linear carbonate electrolyte. In the case of the C-rate capability, EC-EMC and EC-DMC are very similar in rate capability but the EC-DEC showed low discharge capacity compared with EC-EMC and EC-DMC which is mainly attributed to the much higher viscosity. Fig. 3 shows the charge-discharge profile of C-rate with linear carbonate. Similar behavior can be observed on EC-DMC and EC-EMC from the charge-discharge profile but EC-DEC clearly exhibits a high over-potential at the 4.0C and 5.0C than EC-DMC and EC-EMC. After the C-rate capability test, cycling stability tests were employed under a 0.5C in the following order: EC-DMC > EC-EMC > EC-DEC. This result is related to the high viscosity of EC – DEC compared with EC-DMC and EC-EMC, as shown in table 5. Besides, the poor cycle performance and C-rate capability at the high voltage of 5.3 V was previously reported [30], and this study explained that EC-DMC have better C-rate performance and cycle performance because of ionic conductivity. And, DMC is more stable than EMC and DEC because DMC has a high oxidation potential compared with EMC and DEC. As shown in table 5, DMC have lower homo energy than EMC and DEC. Having high homo energy relates to the tendency for oxidation of the electrolyte.

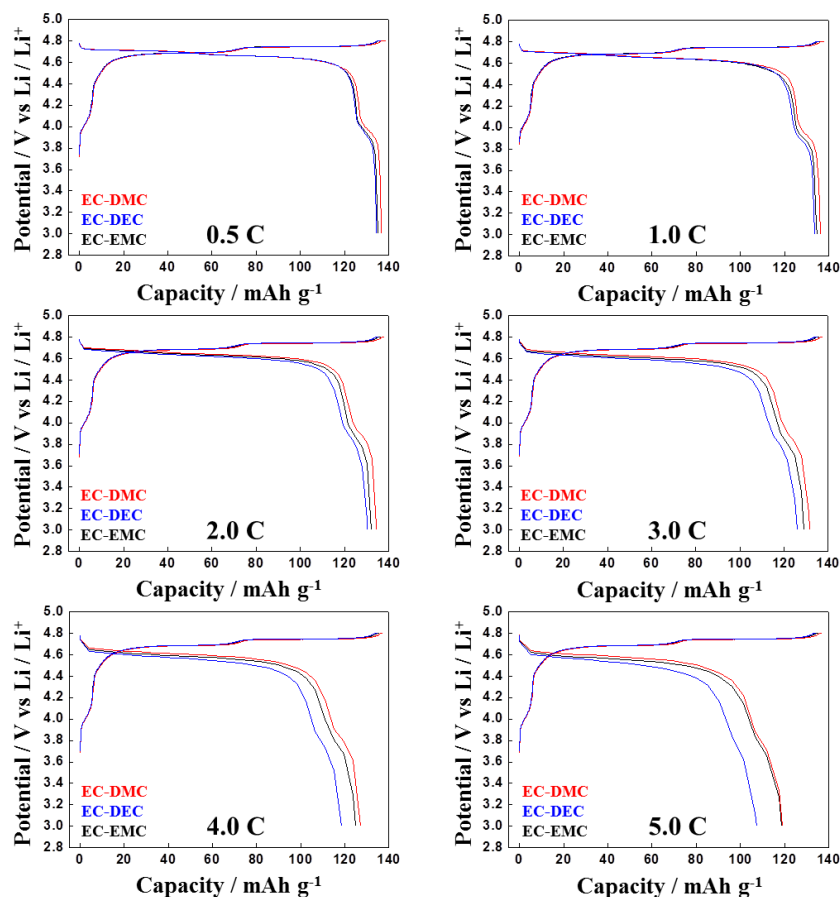


Fig. 3. The charge-discharge profiles of LNMO/Li metal half cells with different C-rate and linear carbonates

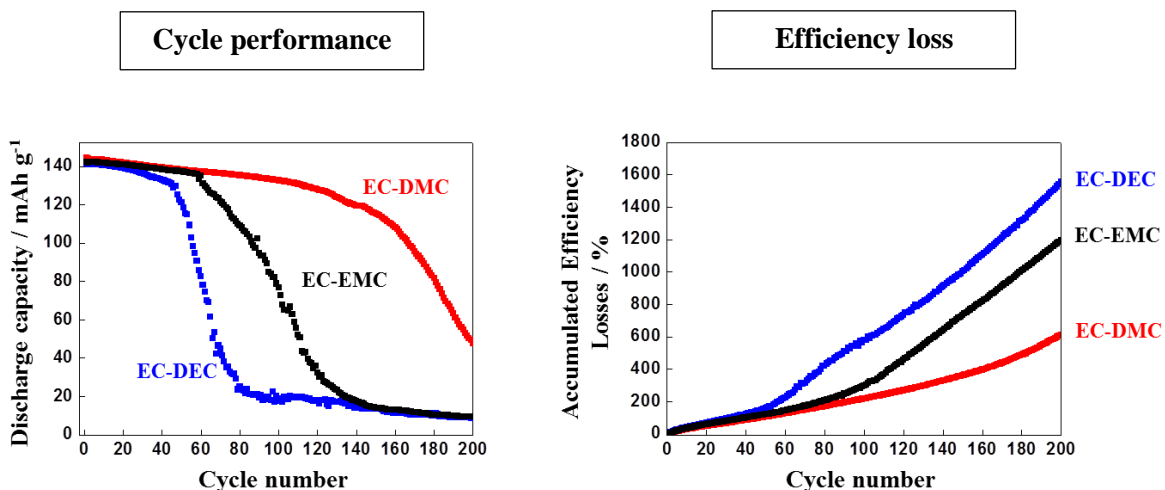
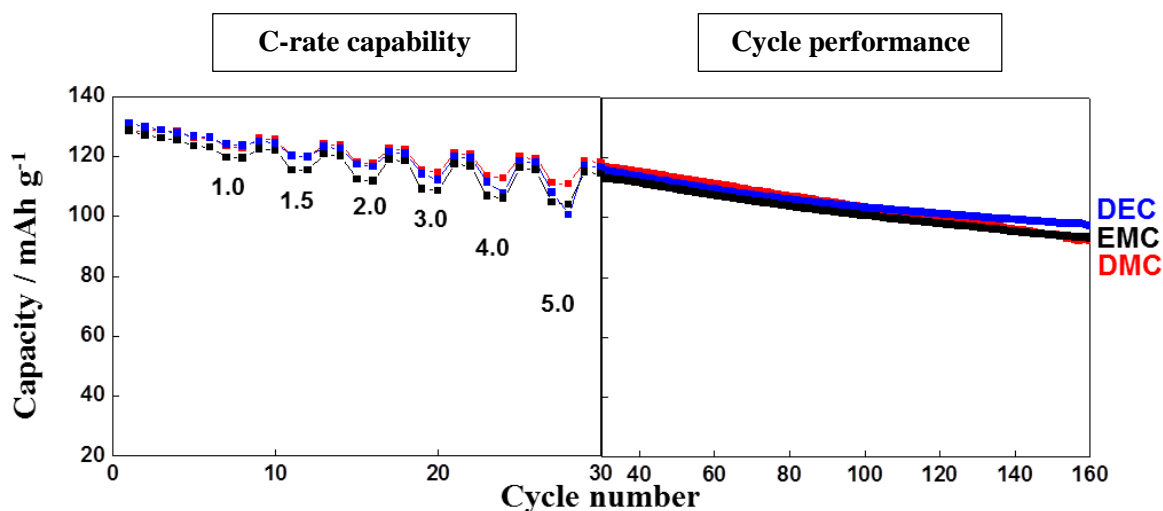


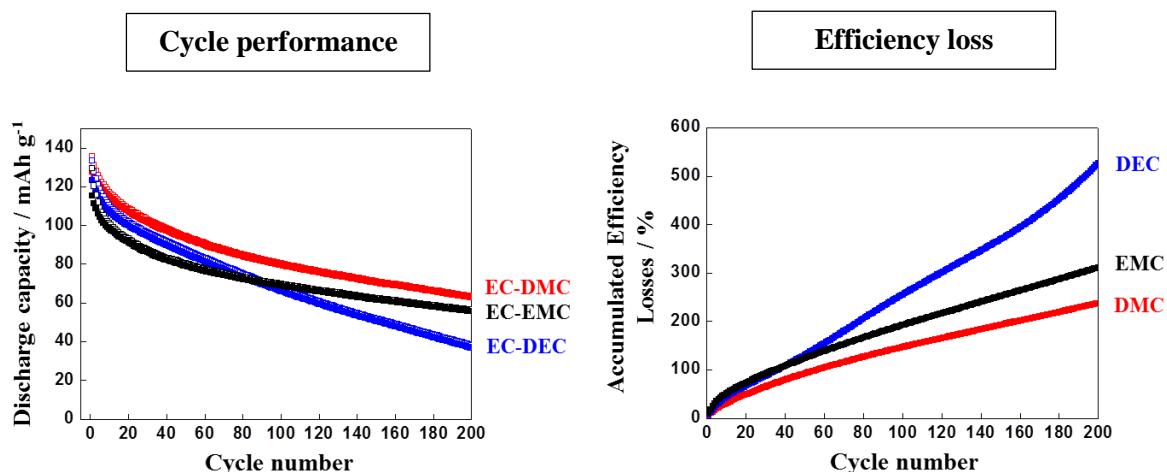
Fig. 4. LNMO / Li metal half-cell performance and accumulated efficiency losses at 55°C with linear carbonates

Fig. 4 shows cycle performance and accumulated efficiency losses of LNMO / Li metal cells at 55 °C. Moreover, EC-DMC exhibits great cycle performance and charge-discharge efficiency compared with EC-EMC and EC-DEC at a high temperature of 55 °C, which is consistent with the result at 25 °C. As mentioned earlier, this result can be explained by the ionic conductivity and oxidation potential of EC-DMC.



**Fig. 5. LNMO / Graphite full-cell C-rate performance at each rate and 0.5C cycle performance at 25 °C with linear carbonates**

After LNMO / Li metal half-cell test, LNMO / Graphite full-cell tests were carried out to evaluate full-cell performance with linear carbonates at room (25 °C) and high (55 °C) temperatures. Fig. 5 shows the C-rate capability and the cycle performances of the LNMO / Graphite cells at 25°C with linear carbonates. EC-DMC composition has better performance than other compositions in the high C-rate but in the cycle performance, all carbonates exhibit similar behavior. However, EC-DMC composition shows great performance of cyclic stability and charge-discharge efficiency compared with EC-EMC and EC-DEC compositions. This result is equivalent with half-cell and means that EC-DMC composition clearly improves the LNMO performance.



**Fig. 6. LNMO / Graphite full-cell performance and accumulated efficiency losses at 55°C with linear carbonate**

### 3.2 The effect of the linear carbonates on self-discharge test

The variation of the open circuit voltage is due to a lithium reinsertion from the electrolyte [32, 33]. Fig. 7 presents the self-discharge profiles at a high temperature of 60 degrees Celsius. As shown in Fig.7, the potential of every cell decreased rapidly to 4.73 V. In the EC-DEC, the electrolytes tend to oxidatively decompose on the charged LNMO, suggesting that it shows the serious potential drop compared with EC-DMC and EC-EMC. However, in case of the EC-DMC, best performance was observed during the self-discharge test. As shown in the table 2, the time of the voltage drop to 4.2 V was 275 hours longer than EC-EMC. This result clearly shows that EC-DMC composition is more stable than EC-EMC and EC-DEC at a high potential range (~4.85 V).

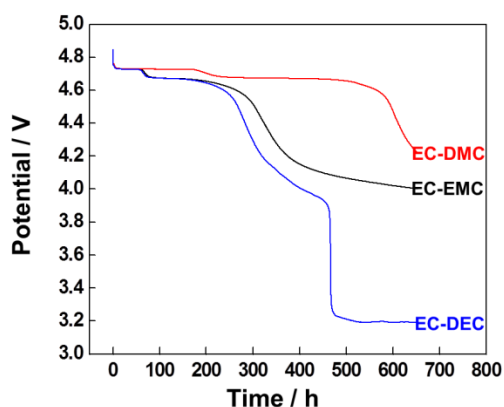


**Fig. 7. Open circuit of voltage evolution of four LNMO half cells with EC-DMC, EC-EMC, and EC-DEC**

	EC-DMC	EC-EMC	EC-DEC
Time to 4.2 V (Self-discharge)	650 h	375 h	320 h
Potential at 160h	4.2 V	4.0 V	3.2 V

**Table 2. Self-discharge comparison of time to potential**

### 3.3. Surface composition analysis of LNMO electrodes with linear carbonates

To better understand the mechanism of linear carbonate on LNMO, the surface compositions of the LNMO cathode were analyzed by using X-ray photoelectron spectroscopy (XPS) after 200 cycles at 55 °C. LNMO / Li metal cells were disassembled and LNMO electrodes were washed with pure dimethyl carbonate.

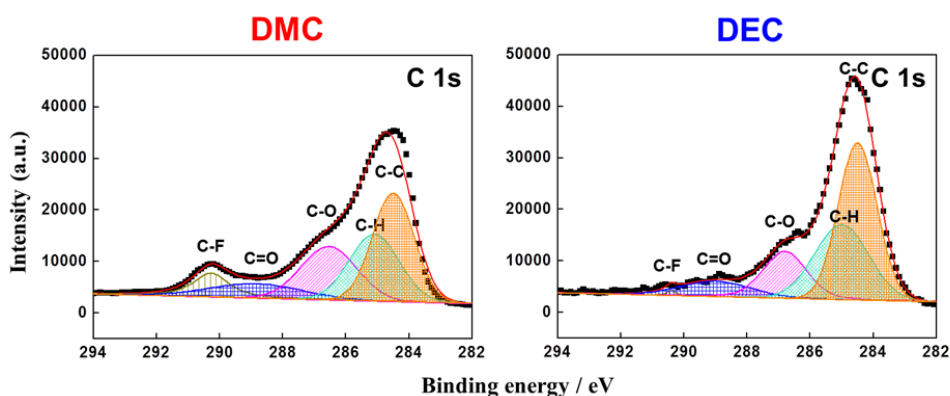


**Fig. 8. XPS C 1s spectra of the LNMO half cells with EC-DMC and EC-DEC after 200 performance cycles at 55°C**

In the C 1s spectra, the peak located at 284.4 eV is assigned to conductive carbon (Super .P), and the peaks at 290.3 eV and 285.0 eV correspond to PVDF. [34, 35] C-O and C=O groups are



located at the 286.5 eV and 288.9 eV, respectively. DEC exhibits a C-F peak smaller than DMC and this can be explained from the electrolyte decomposition and side reaction products on the electrode surface. [36, 37]

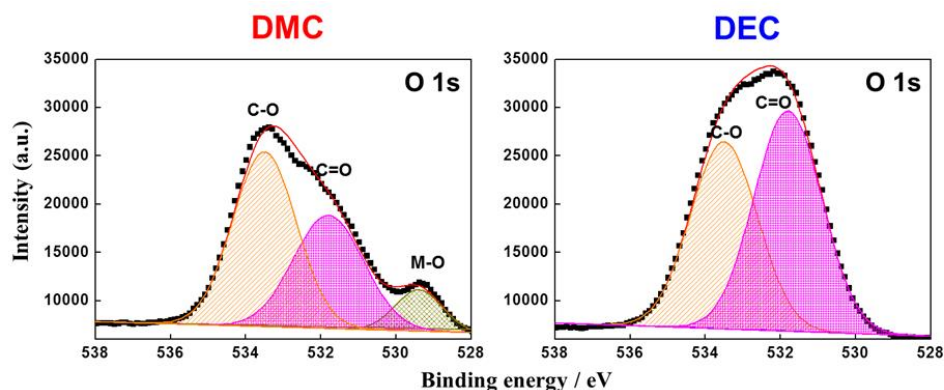


**Fig. 9.** XPS O 1s spectra of LNMO half cells with EC-DMC and EC-DEC after 200 performance cycles at 55°C

The O 1s spectra at 529.4 eV, 531.8 eV and 533.5 eV correspond to metal oxide,  $\text{Li}_2\text{CO}_3$  and lithium alkyl carbonates, respectively. [38, 39] The metal oxide peak (529.4 eV) was not detected which is the result of the decomposition products in the EC-DEC electrolyte.

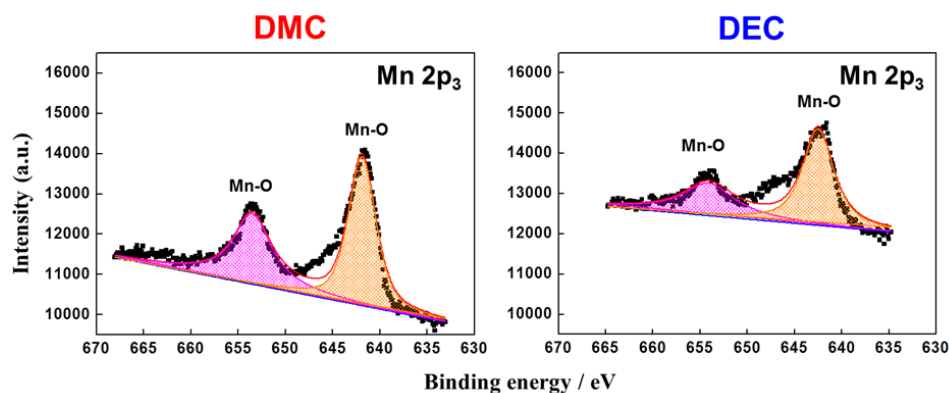


**Fig. 10.** XPS Mn 2 p<sub>3</sub> spectra of the LNMO half cells with EC-DMC and EC-DEC after 200 cycle performance cycles at 55°C

In Mn 2p spectra, manganese oxide peaks were assigned at 653.6 eV and 641.8 eV ( $2p^{3/2}$  and  $2p^{1/2}$ ). [40] The Mn 2p peaks were stronger for the LNMO electrode in the EC-DMC electrolyte than the EC-DEC. The Mn 2p spectra contributed much to the electrolyte decomposition products on the electrode cycled in the EC-DEC electrolyte.

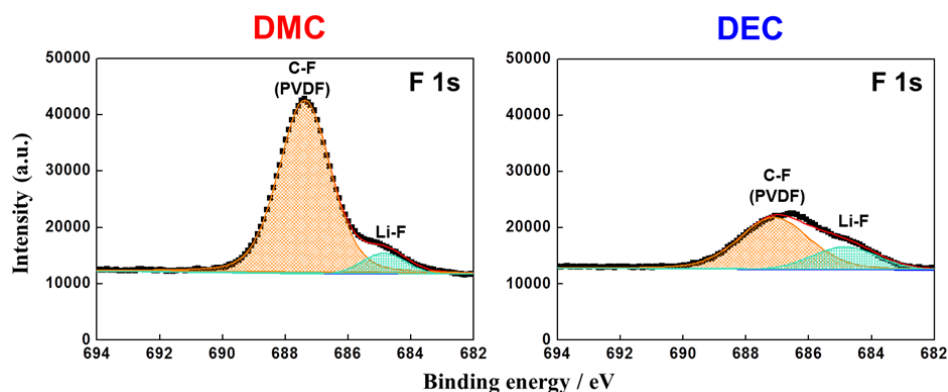


**Fig. 11. XPS Mn 2 p<sub>3</sub> spectra of the LNMO half cells with EC-DMC and EC-DEC after 200 performance cycles at 55°C**

In the F 1s spectra, the peak located at 687.4 eV was attributed to PVDF and the peak at 684.9 eV was assigned to LiF from the decomposition of the salt in the electrolyte [41, 42].

Fig 12 shows the P 2p spectra of the LNMO surface in the EC-DMC and EC-DEC electrolyte. Analysis of the P 2p spectrum suggests that the peaks are consistent with the presence of  $\text{Li}_x\text{PF}_y$  (134.0eV) and  $\text{Li}_x\text{PO}_y\text{F}_z$  (131.2eV). [20] The intensities of  $\text{Li}_x\text{PF}_y$  and  $\text{Li}_x\text{PO}_y\text{F}_z$  peaks of the electrode cycled in the EC-DEC electrolyte are much stronger than the EC-DMC electrolyte, confirming the dramatic decomposition of the EC-DEC electrolyte. [43]

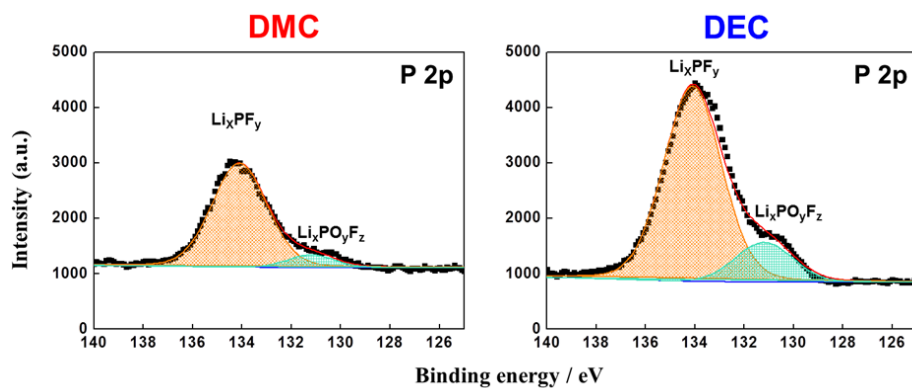


**Fig. 12. XPS P 2p spectra of the LNMO half cells with EC-DMC and EC-DEC after 200 performance cycles at 55 °C**

### 3.4. $\text{LiNi}_{0.5}\text{Mn}_{1.5}\text{O}_4$ / lithium foil cell EIS test

The improved cycle performance from the EC-DMC electrolyte can be further examined by electrochemical impedance spectroscopy (EIS) measurement. Fig 13 presents the electrochemical impedance spectra of the LNMO cathode after high temperature (55 °C) cycle performance testing.

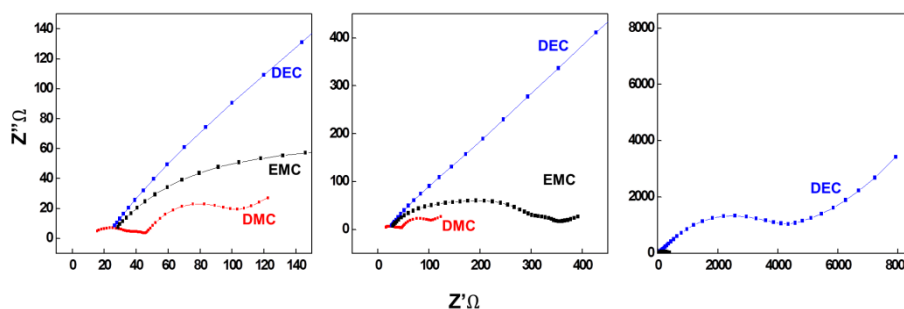


**Fig. 13. Electrochemical impedance spectra of LNMO / Li cells in EC-DMC, EC-EMC, and EC-DEC electrolyte after 200 performance cycles tests at 55°C**

The semicircle reflects the interfacial properties between the LNMO cathode and electrolyte, while the slope line represents the diffusion of lithium ion in the electrode. [44] The reaction resistance for lithium insertion/de-insertion can be estimated by the diameter of the semicircle. [45] As shown in Fig 13, the electrode cycled in the EC-DEC electrolyte shows larger impedance than that cycled in EC-DMC and EMC electrolytes after 200 performance cycles at 55°C. It indicates the instability of the LNMO/electrolyte interface due to electrolyte decomposition.

### 3.5. Linear carbonate effect of HF formation at high temperature (60°C)

To confirm origination of different LC performance, electrolytes were stored at the 60 °C for 10 days to check amount of HF. Before the storage at 60 °C, EC-DMC composition was measured in highest HF concentration among the linear carbonate. However, the electrolyte that was measured in highest increase was EC-DEC composition. This result corresponds to previous study [46] that difference of HF formation from the linear carbonates influence degradation of LNMO. And, this factor contributes to LNMO of electrochemical performance.

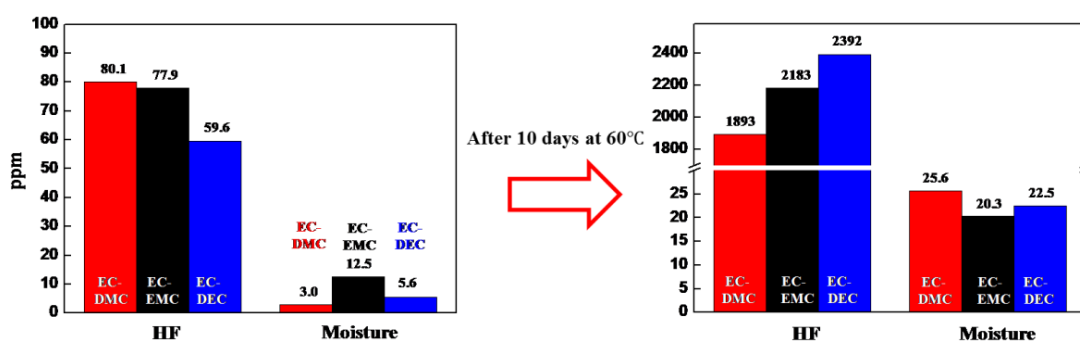


Fig.14. The concentration of HF and moisture before and after high temperature storage with linear carbonates

## 4. Conclusion

The effects of the type of linear carbonates (LC: DMC, DEC, EMC) in 1M LiPF<sub>6</sub> EC / LC (3/7, v/v) were investigated. It was found that the electrochemical performances of LNMO cathode depend on the type of linear carbonate. EC/DMC exhibits superior cyclability and coulombic efficiency at 25 °C and 55 °C than those EC/EMC and EC/DEC. The cells with EC/DMC also show better self-discharge performance than other compositions. The improved electrochemical performances in EC/DMC are attributed to the diminished HF formation compared to the others. This factor affects electrolyte decomposition and manganese dissolution. As a result, the electrochemical stability of LNMO is strongly related to the linear carbonate and EC-DMC composition was found to be most stable.

## Reference

- [1] D. Lu, M. Xu, L. Zhou, A. Garsuch, B.L. Lucht, *Journal of the Electrochemical Society*, 160 (2013) A3138-A3143.
- [2] J. Xiao, X. Chen, P.V. Sushko, M.L. Sushko, L. Kovarik, J. Feng, Z. Deng, J. Zheng, G.L. Graff, Z. Nie, D. Choi, J. Liu, J.G. Zhang, M.S. Whittingham, *Advanced materials*, 24 (2012) 2109-2116.
- [3] Z. Chen, S. Qiu, Y. Cao, X. Ai, K. Xie, X. Hong, H. Yang, *Journal of Materials Chemistry*, 22 (2012) 17768.
- [4] J.-T. Han, J.B. Goodenough, *Chemistry of Materials*, 23 (2011) 3404-3407.
- [5] H.G. Jung, M.W. Jang, J. Hassoun, Y.K. Sun, B. Scrosati, *Nature communications*, 2 (2011) 516.
- [6] S. Komaba, M. Watanabe, H. Groult, N. Kumagai, K. Okahara, *Electrochemical and Solid-State Letters*, 9 (2006) A130.
- [7] Q.-C. Zhuang, J. Li, L.-L. Tian, *Journal of Power Sources*, 222 (2013) 177-183.
- [8] S. Zhang, *Electrochemistry Communications*, 5 (2003) 979-982.
- [9] Y. Zhang, Y. Gui, X. Wu, H. Feng, L. Wang, A. Zhang, X. Li, T. Xia, L. Zhang, P. Zhang, C. Zhang, *Electrochemical and Solid-State Letters*, 12 (2009) A120.
- [10] H. Zheng, Y. Fu, H. Zhang, T. Abe, Z. Ogumi, *Electrochemical and Solid-State Letters*, 9 (2006) A115.
- [11] S. Komaba, M. Watanabe, H. Groult, N. Kumagai, *Carbon*, 46 (2008) 1184-1193.
- [12] B. Wu, Y. Ren, D. Mu, X. Liu, F. Wu, *Journal of Power Sources*, 272 (2014) 183-189.
- [13] P. Bonnick, J.R. Dahn, *Journal of the Electrochemical Society*, 159 (2012) A981-A989.

- [14] M.D. Stoller, S.A. Stoller, N. Quarles, J.W. Suk, S. Murali, Y. Zhu, X. Zhu, R.S. Ruoff, *Journal of Applied Electrochemistry*, 41 (2011) 681-686.
- [15] S.S. Zhang, K. Xu, T.R. Jow, *Journal of Solid State Electrochemistry*, 7 (2003) 492-496.
- [16] S. Krueger, R. Kloeppsch, J. Li, S. Nowak, S. Passerini, M. Winter, *Journal of the Electrochemical Society*, 160 (2013) A542-A548.
- [17] M. Xu, Y. Liu, B. Li, W. Li, X. Li, S. Hu, *Electrochemistry Communications*, 18 (2012) 123-126.
- [18] B. Wu, Y. Ren, D. Mu, X. Liu, G. Yang, F. Wu, *RSC Advances*, 4 (2014) 10196.
- [19] B. Li, Y. Wang, W. Tu, Z. Wang, M. Xu, L. Xing, W. Li, *Electrochimica Acta*, 147 (2014) 636-642.
- [20] S. Mai, M. Xu, X. Liao, J. Hu, H. Lin, L. Xing, Y. Liao, X. Li, W. Li, *Electrochimica Acta*, 147 (2014) 565-571.
- [21] H. Lee, J.-J. Cho, J. Kim, H.-J. Kim, *Journal of The Electrochemical Society*, 152 (2005) A1193.
- [22] M. Morita, T. Shibata, N. Yoshimoto, M. Ishikawa, *Journal of Power Sources*, 119-121 (2003) 784-788.
- [23] M.S. Ding, K. Xu, S.S. Zhang, K. Amine, G.L. Henriksen, T.R. Jow, *Journal of The Electrochemical Society*, 148 (2001) A1196.
- [24] M.I. Soon-Ki Jeong, Yasutoshi Iriyama, Takeshi Abe, Zempachi Ogumi, *Electrochimica Acta*, 47 (2002) 1975-1982.
- [25] D.L. Julien Demeaux\*, Hervé Galiano, Magaly Caillon-Caravanier, Bénédicte Claude-Montigny,, *Electrochimica Acta*, 116 (2014) 271-277.
- [26] D.-T.S. Fu-Ming Wang, Ju-Hsiang Cheng, Chang-Rung Yang, *Solid State Ionics*, 180 (2010) 1660-1666.

- [27] S.O. Tetsuya Kawamura\*, Jun-ichi Yamaki, *Journal of Power Sources*, 156 (2006) 547-554.
- [28] T.R.J. S.S. Zhang\*, K. Amine, G.L. Henriksen, *Journal of Power Sources*, 107 (2002) 18-23.
- [29] E.R. Hongsen Wang, Takahito Sakuraba, Jun Kikuchi, Yasuyuki Kiya, and Héctor D. Abruña, *American Chemical Society*, 86 (2014) 6197-6201.
- [30] W. Xu, X. Chen, F. Ding, J. Xiao, D. Wang, A. Pan, J. Zheng, X.S. Li, A.B. Padmaperuma, J.-G. Zhang, *Journal of Power Sources*, 213 (2012) 304-316.
- [31] D.L. Julien Demeauxa\*, Magaly Caillon-Caravanier, Hervé Galiano, Bénédicte Claude-Montigny, *Electrochimica Acta*, 89 (2013) 163-172.
- [32] R. Yazami, Y. Ozawa, *Journal of Power Sources*, 153 (2006) 251-257.
- [33] e.a. G. Pistoia, *Electrochimica Acta*, 41 (1996) 2683-2689.
- [34] X. Cao, Y. Li, X. Li, J. Zheng, J. Gao, Y. Gao, X. Wu, Y. Zhao, Y. Yang, *ACS applied materials & interfaces*, 5 (2013) 11494-11497.
- [35] M. Xu, L. Hao, Y. Liu, W. Li, L. Xing, B. Li, *The Journal of Physical Chemistry C*, 115 (2011) 6085-6094.
- [36] M. Xu, L. Zhou, Y. Dong, Y. Chen, A. Garsuch, B.L. Lucht, *Journal of the Electrochemical Society*, 160 (2013) A2005-A2013.
- [37] B. Wang, Q.T. Qu, Q. Xia, Y.P. Wu, X. Li, C.L. Gan, T. van Ree, *Electrochimica Acta*, 54 (2008) 816-820.
- [38] W. Li, A. Xiao, B.L. Lucht, M.C. Smart, B.V. Ratnakumar, *Journal of The Electrochemical Society*, 155 (2008) A648.
- [39] G. Liu, Y. Li, B. Ma, Y. Li, *Electrochimica Acta*, 112 (2013) 557-561.

- [40] R. Dedryvère, S. Laruelle, S. Grugeon, L. Gireaud, J.M. Tarascon, D. Gonbeau, *Journal of The Electrochemical Society*, 152 (2005) A689.
- [41] A.M. Andersson, D.P. Abraham, R. Haasch, S. MacLaren, J. Liu, K. Amine, *Journal of The Electrochemical Society*, 149 (2002) A1358.
- [42] S. Wilken, M. Treskow, J. Scheers, P. Johansson, P. Jacobsson, *RSC Advances*, 3 (2013) 16359.
- [43] C.F. Xiaoxi Zuo, Xin Xiao, Jiansheng Liu, Junmin Nan\*, *Journal of Power Sources*, (2012) 94-99.
- [44] W. Huang, L. Xing, Y. Wang, M. Xu, W. Li, F. Xie, S. Xia, *Journal of Power Sources*, 267 (2014) 560-565.
- [45] V. Tarnopolskiy, J. Kalhoff, M. Nádherná, D. Bresser, L. Picard, F. Fabre, M. Rey, S. Passerini, *Journal of Power Sources*, 236 (2013) 39-46.
- [46] J.C. Simon Franz Lux\*, Ivan T. Lucas and Robert Kostecki\*\*, *ECS Electrochemistry Letters*, (2013) A121-A123.
- [47] C.-H.H. Jee-Sun Shin, Un-Ho Jung, Shung-Ik Lee, Hyeong-Jin Kim, Keon Kim, *Journal of Power Sources*, 109 (2002) 47-52.
- [48] L.J.K. J. C. Burns\*, Dinh-Ba Le, L. D. Jensen, A. J. Smith, Deijun Xiong, and J. R. Dahn, *Journal of The Electrochemical Society*, 158(12) (2011) A1417-A1422.
- [49] D.O. E. Wang, W. Bowden\*, N. Ilchev\*, Moses, and K. Brandt\*, *Journal of The Electrochemical Society*, 147 (11) (2000) 4023-4028.
- [50] Y.-C.L. Ronald A. Quinlan, Yang Shao-Horn, and Azzam N. Mansour, *Journal of The Electrochemical Society*, 160(4) (2013) A669-A677.



## 요약문

### Alkali carbonates 첨가제와 전해액 조성이 $\text{LiNi}_{0.5}\text{Mn}_{1.5}\text{O}_4$ 양극의 전기화학적 성능에 미치는 영향

리튬 이차전지에서 사용되는 5 V 급 양극재인  $\text{LiNi}_{0.5}\text{Mn}_{1.5}\text{O}_4$  (이하 LNMO)는 높은 구동전압과 낮은 가격, 합리적인 용량으로 인해  $\text{LiCoO}_2$  를 대체 할 양극 물질로 각광받고 있다. 그러나 고전압에서의 전해액분해와 양극 물질로부터 Ni 과 Mn 이온의 용출은 전지의 성능저하와 수명특성을 감소시키는 문제를 발생시키고, 이러한 문제를 해결하기 위해 다양한 연구들이 진행되어 왔다. 본 논문에서는 LNMO 의 수명특성과 충방전 효율향상을 위해 첨가제와 전해액조성에 관한 연구를 진행하였다.

첫 번째로, alkali carbonates ( $\text{CaCO}_3$ ,  $\text{MgCO}_3$ ,  $\text{Li}_2\text{CO}_3$ )를 전극첨가제와 전해액첨가제로 이용하여 전해액내의 HF 를 감소시킴으로써, LNMO 의 충방전 효율과 수명특성을 개선하였다. 각 첨가제의 효과를 확인하기 위해 Coin-type cell test 를 상온(25 °C)과 고온(55, 60 °C)에서 진행되었고,  $\text{CaCO}_3$  가 전극 및 전해액 첨가제 모두에서 고온 수명 특성 및 충방전 효율을 향상시키는 효과가 있었다. 이어서, 첨가제가 HF 를 효과적으로 억제하는지의 여부를 확인하기 위해 CV test 와 XPS 분석을 실시하였다. 그 결과  $\text{CaCO}_3$  가 포함 된 전해액에서 HF 를 효과적으로 억제하는 것을 확인할 수 있었다.

두 번째로, Linear carbonate(LC)에 따른 LNMO 의 수명특성과 충방전 효율을 비교하였다. 전해액 구성은 Ethylene carbonate 와 LC(DMC, DEC, EMC)를 3:7(v/v)로 구성하여, Coin half cell 과 full cell test 를 통해 상온(25 °C)과 고온(55, 60 °C)에서 수명특성과 효율, C-rate capability 를 확인하였다. C-rate capability(25°C)의 경우 EC-DMC 와 EC-EMC 조합에서 유사한 성능을 보였지만 수명특성과 효율에서는 상온과 고온 모두에서 EC-DMC 가 EC-EMC 와 EC-DEC 에 비해 우수한 성능을 보였다. 또한 자가방전(60°C) test 에서도 coin half cell 과 full cell 모두에서 EC-DMC 가 가장 우수한 성능을 나타냈다. 이러한 결과는 각 linear carbonate 에 따른 부반응의 차이로부터 기인한 것이라 생각되며, 이를 EIS 와 XPS 표면분석을 통해 확인 할 수 있었다. 또한 각 조성의 전해액을 고온 보존함으로써 보존 전 후의 HF 생성량을 분석한 결과  $\text{DEC} > \text{EMC} > \text{DMC}$  순으로 HF 생성량이 증가하는 것을 확인할 수 있었다. 이는 앞서 언급한 coin-type cell test 결과와도 일치하며 각 linear carbonate 에 따라 생성된 HF 로부터 LNMO 의 열화가 촉진되어 성능 차이에 기인한 것을 확인할 수 있었다.

핵심어: Li-ion batteries,  $\text{LiNi}_{0.5}\text{Mn}_{1.5}\text{O}_4$ , HF, alkali carbonate, additive, linear carbonate